2009-01-1956

Multi-Zone DI Diesel Spray Combustion Model for Thermodynamic Simulation of Engine with PCCI and High EGR Level

A.S. Kuleshov
Bauman Moscow State Technical University

ABSTRACT

A multi-zone, direct-injection (DI) diesel combustion model, the so-called RK-model, has been developed and implemented in a full cycle simulation of a turbocharged engine. The combustion model takes into account:

- transient evolution of fuel sprays,
- interaction of sprays with swirl and walls,
- evolution of near-wall flow formed after spray-wall impingement depending on impingement angle and local swirl velocity,
- interaction of Near-Wall Flows (NWF) formed by adjacent sprays,
- influence of temperatures of gas and walls in the zones on evaporation rate.

In the model the fuel spray is split into a number of specific zones with different evaporation conditions including zone on the cylinder liner and on the cylinder head. The piston bowl is assumed to be a body of revolution with arbitrary shape. The combustion model supports central and non-central injector as well as the side injection system. NOx formation model uses Detail Kinetic Mechanism (199 reactions with 33 species). Soot formation model is phenomenological. The general equation for prediction of ignition delay period was derived as for conventional engines as for engines with PCCI where pilot injection timing achieved 130 CA deg. before TDC. The model has been validated by experimental data obtained from high-speed, medium-speed and low-speed engines over the whole operating range; a good agreement has been achieved without recalibration of the model for different operating modes.
General equations for prediction of spray tip penetration, spray angle and ignition delay for low temperature combustion and high temperature combustion were derived and validated with the published data obtained for different diesels including diesels with multiple injection system and injection timing varied from very early up to after the TDC.
To make a computational optimization of multiple injection strategy possible, the full cycle thermodynamic engine simulation software DIESEL-RK has been supplied with library of nonlinear optimization procedures.

INTRODUCTION

The combustion process as well as NOx and PM emissions formation in direct-injection diesels are very sensitive to engine parameters such as the sprayer design and location, the piston bowl shape, swirl intensity, strategy of EGR use, and injection profile including multiple electronic controlled injection.

One area that still holds potential for lowering NOx emissions within the engine is the modification of the combustion process so that more of the combustion occurs under lean conditions, which reduces local combustion temperatures and NOx formation. Lowering combustion temperature allows simultaneously reduce NOx and soot formation. One method of achieving overall lean combustion is Premixed Charge Compression Ignition (PCCI) or Homogeneous Charge Compression Ignition (HCCI) where the entire fuel and air charge is premixed prior to the start of combustion. PCCI/HCCI has been the focus of numerous researches due to its potential for extremely low NOx without increases in PM or fuel consumption. Due to the high rate of pressure rise and problems with controlled start of combustion there are challenges of use the PCCI/HCCI operation over the full engine operating range. So at computational analysis of an engine the mathematical model and computer code have to support both the conventional engine combustion and PCCI/HCCI combustion without discontinuity to make it possible the computer optimization of engine control parameters over the whole engine operating range.

Due to a great number of available options and their combinations, a search for the optimal solution is a long and labor-consuming task. Simulation as well as computational optimization can effectively to point out trends and effective ways of engine improvement.

There are nowadays three categories of diesel engine simulation models:

- Zero-dimensional single-zone models;
- Quasi-dimensional multi-zone models;
- Multi-dimensional models (CFD).

Although CFD possesses, in principle, the ability to simulate all fluid-flow/heat-transfer/chemical-reaction phenomena, in practice it is limited by: a) the limited capability of current computers to handle small-scale phenomena in an acceptably short time; b) the inadequacy of current scientific knowledge about turbulence, two-phase flow and chemical reaction, especially when all three are simultaneously presented. So, the attempt to optimize diesel-engine processes by way of 'pure CFD' cannot be succeeded at present.

The choice of the thermodynamic engine model together with quasi-dimensional multi-zone model of combustion accounting peculiarities of conventional and PCCI diesel combustion is conditioned by requirements of high accuracy and the high computational speed, because the number of engine simulation sessions in optimization over the whole operating range comes up to few thousands.

The earlier published multi-zone diesel spray combustion model [1, 2, 3], named the RK-model includes three independent emission submodels: the NOx formation submodel based on the Zeldovich's scheme [4] developed by Zvonov [5]; the soot formation submodel developed by Razleytsev [6]; the advanced NOx formation submodel based on Detail Kinetic Mechanism (DKM) for correct prediction of NO emission in engine with large EGR, multiple injection and PCCI/HCCI. DKM includes 199 reactions with 33 species, one was built on the kinetic scheme by prof. Basevich V.J. [5, 7, 8, 9]. Soot and NOx formation processes are simulated with separate procedures after combustion modeling. The main equations of the RK-model were derived by Razleytsev in 1990-1994. This method afterwards was modified and complemented by Kuleshov [1, 2, 3].

The RK-model takes into account conditions of evolution of each fuel spray and near-wall flows generated by sprays; and also interaction between sprays and swirl, as well as between near-wall flows, formed by adjacent sprays. These features of the RK-model allow prediction of diesel combustion and emissions over the whole operating range for the following varying parameters:

- piston bowl shape and sprayer location;
- swirl intensity;
- number, diameter and direction of sprayer nozzles;
- injection profile shape and any multiple injection.

A more detailed description of the RK-model was given in [1, 2, 3, 53]. The present paper describes the same model with peculiarities being implemented to improve accuracy of heat release prediction in diesels with PCCI.

GENERAL PRINCIPLES OF SPRAY MODELLING

The theoretical background of the model is based on the method developed in [6] in which the fuel spray injected into the combustion chamber of the engine is split into a number of specific zones. This is caused by the necessity of detailed account for following fuel spray evolution peculiarities:

- difference of fuel droplet evaporation conditions in different spray zones;
- fuel redistribution among zones in the process of free spray movement and in its interaction with a wall;
- interaction of fuel sprays with the walls of the piston bowl and possibility of fuel hitting the cylinder liner and the cylinder head surface;
- effect of the wall temperature on the fuel evaporation rate in near-wall zones;
- interaction of adjacent sprays in near-wall flows.

The spray evolution passes through three stages:

- Initial formation of dense axial flow.
- Main stage of cumulative spray evolution.
- Period of spray interaction with the combustion chamber walls and fuel distribution on the walls.

Liquid spray breakup takes place close to the nozzle. High-speed fuel portions move quickly towards the spray tip pushing apart, impacting and thus coalescing with droplets formed earlier. In the spray cross section the distribution density of droplets and their diameter reduce rapidly with growing distance from the spray axis. In this context, near the jet boundary droplets are slowed down more rapidly than those near the axis and are gradually delayed and separated from them.

At the main evolution stage later on, the axial flow is slowed down and concentrated on the forward front side because of the surrounding gas resistance. New flying fuel portions reach the axial flow, penetrate inside, push and condense it at the rear. This results in an extended axial core with increased density and droplet velocity being formed in the middle of the spray [10]. This core is surrounded by a relatively dilute outer sleeve made of delayed droplets. Corresponded scheme of diesel fuel spray is presented in Fig. 1.

Figure 1. Scheme of diesel fuel spray, concentration of fuel droplets and its tracks.

The border between the initial and main stages of spray evolution corresponds to the moment when the axial flow close to the spray tip starts to deform and break up, forming a condensed mushroom-shaped forward front. As the spray moves on, constant breakup of the spray forward part [11] takes place and the front is renewed by new flying fuel portions [12, 13]. The delayed droplets move from the breaking front to the environment. The moving spray carries the surrounding gas with it, the gas

velocity in the environment being rather low. Meanwhile gas in the axial core is rapidly accelerated to the velocity close to that of droplets [14]. The core diameter in the cross section is about 0.3 of the spray outside diameter.

In accordance with [6], the current position and the velocity of an Elementary Fuel Mass (EFM) injected during small time-step and moving from the injector to the spray tip are related as

$$\left(\frac{U}{U_o} \right)^{3/2} = 1 - \frac{l}{l_m} \qquad (1)$$

where: l is the current distance between the injector's nozzle and the EFM; $U = dl/dt_k$ is the current velocity of the EFM; t_k is the travel time for the EFM to reach a distance l from the injector's nozzle; U_o is the initial velocity of the EFM at the nozzle of the injector and l_m is the EFM's penetration distance.

As an illustration, Fig. 2 presents the variation of spray evolution parameters l, l_m, U and U_m as functions of time for a medium speed diesel engine.

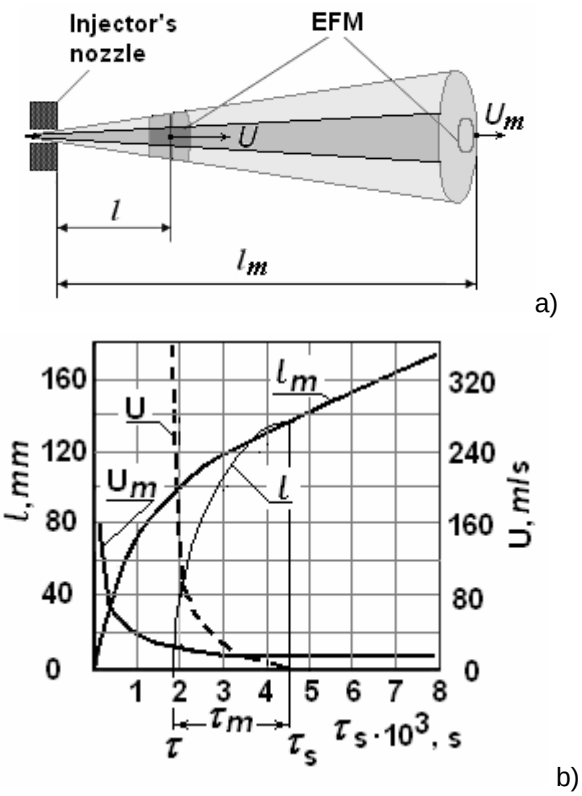

Figure 2. The simplified sketch of the spray (a) and variations of spray evolution parameters: l, l_m, U and U_m as functions of time (b).

Upon termination of fuel evolution there is still some fuel in its axial core supplied at the final injection stage. At the initial combustion stage the flame is unable to break up the fuel spray condensed core [15, 16, 6] which explains why the sprays continue to move to the combustion chamber sidewalls during injection even after fuel ignition. By the end of fuel supply a considerable fraction of the fuel cycle portion is accumulated near the walls. This takes place both in diesels with compact combustion chambers and in engines with wide piston bowls (Hesselman). The interaction of fuel sprays with chamber walls was studied in numerous literature sources [17-24]. Having analyzed various data, Razleytsev proposed the following model of fuel spray interaction with a wall. On reaching the wall, the spray is spread over its surface in every direction. The upward flow over the wall gets quickly into a clearance between the piston and cylinder head and under constricted conditions spreads along the piston crown as well as the cylinder head surface (Fig. 3). A part of fuel can reach the cylinder liner. Analysis of experimental data has shown that characteristics of flows moving along the wall in different directions are similar to those obtained for a freely moving spray, but the velocity level is lower and depends on the flow direction. Reduction in the flow velocity along the wall is caused by the hydrodynamic resistance of the nearby wall.

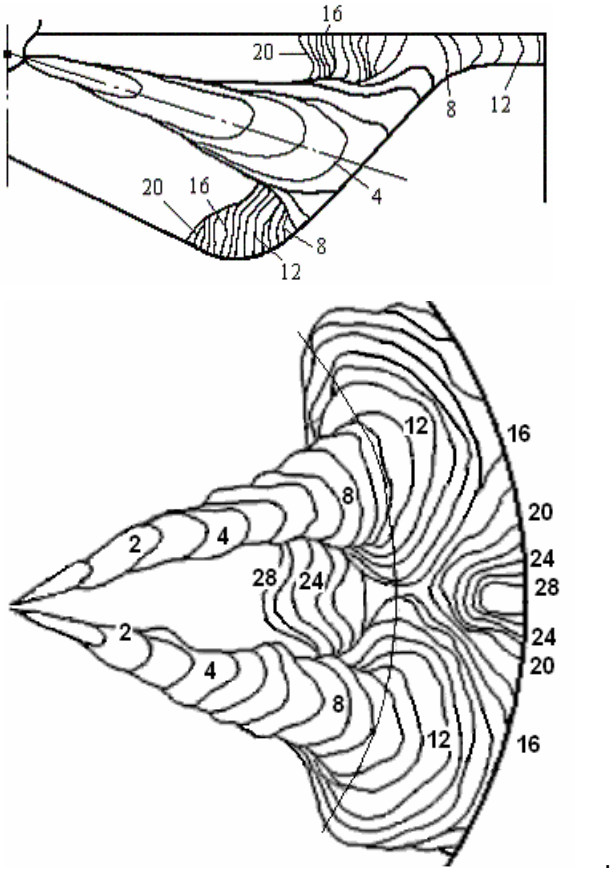

Figure 3. Photo-record obtained by Koptev, Gavrilov [25], Plotnikov. Fuel was injected into the bomb with the piston model. Nozzles: 7 x 0.4 mm. Speed of shooting is 3700 frame/sec. The numbers correspond to frames of shooting.

The mentioned similarity in evolution between near-wall flows and free sprays provides the basis for the application of the same computational procedures to near-wall flows and free sprays. The assumption that the velocity of an elementary fuel portion flying along the wall

is analogous to the fuel outflow velocity from a sprayer makes it possible to apply conventional criterion relations for simulation of the flows in the near-wall zone.

As the spray hits the wall, the forward front fuel enters the near-wall flow zone. The spray trajectory and, therefore, the time, the place and wall impingement angle are determined in view of the swirl effect. The process of spray interaction with a wall is rather complicated. The following scheme of spray and NWF evolution is proposed.

- During the spray forward front impingement with a wall a conical condensed gas-fuel layer is being formed there within the borders of a stain formed at the intersection of a conical spray with the wall surface (zone 4 in the fig. 10).
- On fast fuel spray front impingement with the wall the fuel spreads out of the initial stain limits.
- The high-speed axial flow of a spray in its hitting the wall thickens the near-wall layer, draws apart its borders and a part of the flow moves to its periphery above this layer.
- The shape of the near-wall stain and its spreading rate in various directions depend on the spray-with-the wall impingement angle and the air swirl effect.

A typical photo-record of the evolution of a spray in the combustion chamber is shown in Fig.3.

The partial solution of the differential equation 1 is:

$$3l_m\left[1-\left(1-\frac{l}{l_m}\right)^{0.333}\right]-U_0 t_k = 0 \qquad (2)$$

where t_k is the time of EFM movement from the nozzle up to l. When EFM is stopped in a spray tip $l = l_m$, $t_k = t_m$ and

$$l_m = U_o\ t_m / 3. \qquad (3)$$

From equations 1, 2, 3 it follows:

$$U = U_0\left(1-t_k/t_m\right)^2\ ; \qquad (4)$$

$$l = l_m\left[1-\left(1-t_k/t_m\right)^3\right]\ . \qquad (5)$$

Parameters of the spray tip are calculated with empirical equations of Lyshevsky [26]. These relations use dimensionless criteria:

$$We = U_{0m}^2\, d_n\ r_f / s_f\ ; \qquad (6)$$

$$M = Oh^2 = m_f^2 / \left(r_f\, d_n\, s_f\right)\ ; \qquad (7)$$

$$\Im = t_s^2\, s_f / \left(r_f\, d_n^3\right)\ ; \qquad (8)$$

$$r = r_{air} / r_f \qquad (9)$$

where: U_{0m} is the average injection velocity, d_n is the nozzle hole diameter, r_f is the fuel density, r_{air} is the air density, s_f is the fuel surface density, m_f is the dynamic viscosity coefficient of fuel, t_s is the current time from the injection beginning.

Evolution of a free spray consists of two main phases: a) initial phase of pulsing evolution; b) basic phase of cumulative evolution. The border between these phases is marked as l_g (length) and t_g (time):

$$l_g = C_s\, d_n\, We^{0.25} M^{0.4}\, r^{-0.6}; \qquad (10)$$

$$t_g = l_g^2 / B_s\ ; \qquad (11)$$

$$B_s = d_n\, U_{0m}\, We^{0.21} M^{0.16} / \left(D_s\sqrt{2\ r}\right); \qquad (12)$$

where C_s = 8.25÷8.85; D_s = 4.5÷5 for diesel cylinder conditions. The spray tip penetration length in the initial (index *a*) and the base (index *b*) phases is calculated by the following empirical expressions [6]:

$$l_a = A_s \Im^{0.35}\, exp\left[-0.2\left(t_s/t_g\right)\right]; \qquad (13)$$

$$l_b = B_s^{0.5} t_s^{0.5}; \qquad (14)$$

where: $A_s = 1.22\, l_g\, \Im_g^{-0.35}$ and criterion $\Im_g$ are calculated by equation (8) with the assumption $t_s = t_g$. The form of equation (14) is close to that derived by Kuo [27] and Hiroyasu [28]. Equations (6-14) with D_s = *const* were obtained by Lyshevsky for medium-speed diesels. To make this model suitable for high-speed diesels with small injector nozzles as well, the following expression for D_s was derived in the current investigation:

$$D_s = 14.21 / D_f \qquad (15)$$

where:

$$D_f = \begin{cases} 2.9, & if\ d_n \ge 0.3 \\ 2.9\left(a\cdot d_n^3 + b\cdot d_n^2 + c\cdot d_n + d\right), & if\ d_n < 0.3 \end{cases}; \qquad (16)$$

d_n is the nozzle diameter in millimeters; *a*=9.749; *b*=7.45; *c*=-7.21; *d*=2.224. Equations (15) and (16) have been derived as a result of analysis of experimental data on the dependence of a fuel spray penetration distance from the value of the nozzle diameter and injection pressure published in [29–32]. In these investigations the diameter of the nozzles and injection pressures were varied from 0.11 to 0.45 mm and from 300 to 1200 bar, respectively. The results of this analysis demonstrate that the pressure of the fuel injection does not affect the value of D_s significantly. The variation of D_s as a function of d_n is shown in Fig.4.

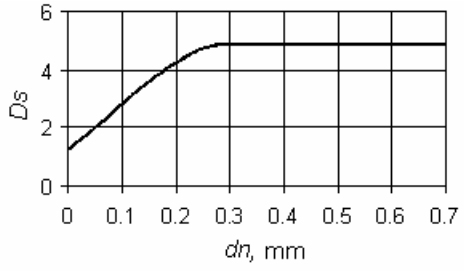

Figure 4. The variation of D_s as function of nozzle diameter d_n.

Comparison between calculated and measured spray tip penetrations for engines with different nozzles hole diameters d_n and different injection pressure values P_{inj} are shown in the Fig.5.

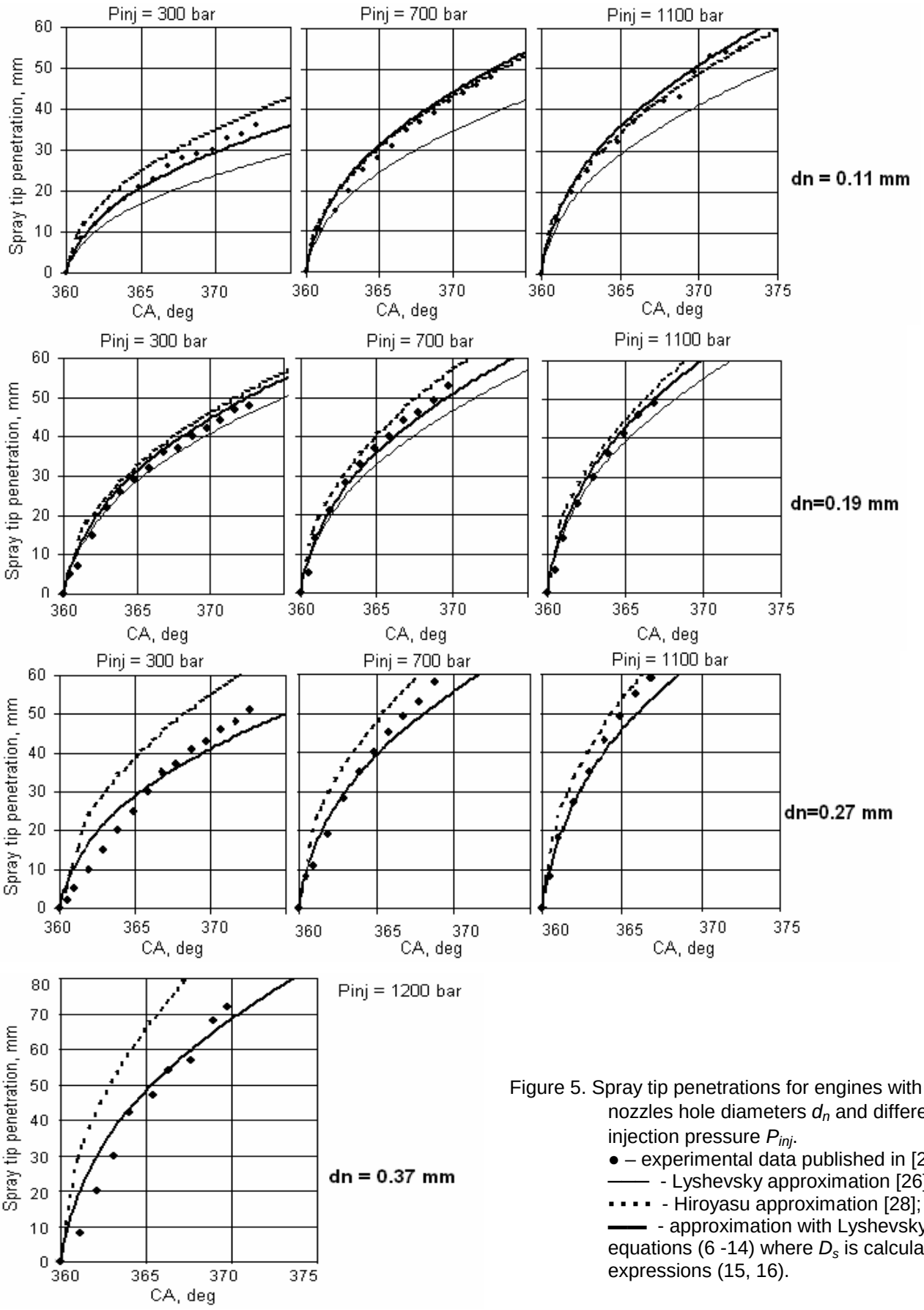

Figure 5. Spray tip penetrations for engines with different nozzles hole diameters d_n and different injection pressure P_{inj}.
● – experimental data published in [29 - 32];
—— - Lyshevsky approximation [26];
▪ ▪ ▪ ▪ - Hiroyasu approximation [28];
▬▬ - approximation with Lyshevsky equations (6 -14) where D_s is calculated with expressions (15, 16).

Presented data show the Hiroyasu approximation is working well at small injector nozzle diameter (d_n<0.25 mm), as well the Lyshevsky approximation [26] gives underrated spray tip penetration at small nozzles diameter. If nozzles diameter exceed 0.25 mm the Hiroyasu approximation overrates spray tip penetration, but the Lyshevsky approximation becomes to be working well. The presented equations (6-16) are general and show correct results over the wide range of spray nozzles diameter variation and at different injection pressures.

The spray angle is calculated as follows:

$$g_a = 2Arctg\left(E_s We^{0.35} M^{-0.07} \Im^{-0.12} r^{0.5} e^{0.07 t_s / t_g}\right); \quad (17)$$

$$g_b = 2Arctg\left(F_s We^{0.32} M^{-0.07} \Im^{-0.12} r^{0.5}\right) \quad (18)$$

where: $E_s = 0.932 F_s We^{-0.03} \Im_g^{0.12}$ and criterion $\Im_g$ are calculated by equation (8) with the assumption $t_s = t_g$, Fs = 0.0075÷0.009 for diesel cylinder conditions. The free spray contour angles obtained by different simulation methods and experimentally are compared in Fig. 6.

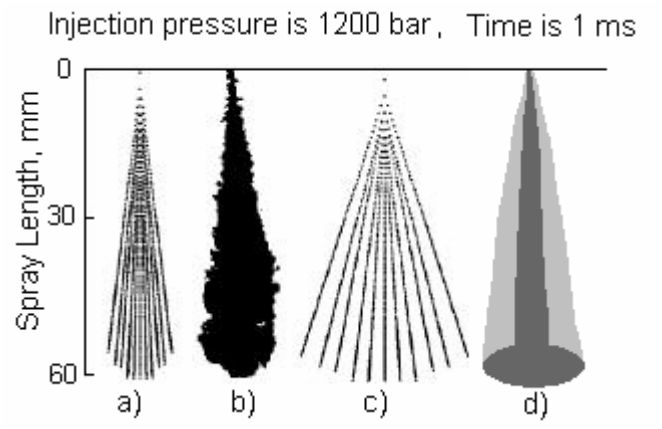

Figure. 6. The free spray contours obtained by different ways: a) calculated with KIVA by Reitz and Bracco [33]; b) measured by Dan [34]; c) calculated by Jung and Assanis [35] using Hiroyasu and Arai equations [36]; d) calculated with equations (17, 18).

If a swirl with angular velocity ω exists in the combustion chamber then the spray is deformed and deflected by some distance *y* in the tangential direction inside the chamber, as shown in Fig. 7. The deformation of the initial conical form of the spray is characterized by the parameters *y, y_3, y_4* and *r*. Local tangential air velocity is:

$$W_t = c\, R_s\, p\, n R / 30; \quad (19)$$

where: R_S = ω / ω_C is the swirl ratio, n is the engine speed, R is the current radius, χ is the swirl damping factor depending on CA. Tangential velocity of EFM in the swirl direction U_t is defined by the equation published in [37]:

$$dU_t / dt = A_{wt}\, W_t^{1.5}; \quad A_{wt} = 0.75 C\, r\, n^{0.5} d_{32}^{-1.5} \quad (20)$$

where: $C \approx 5$ is empirical coefficient, ν is air viscosity, $d_{32} = 1.7\, d_n\, M^{0.0733} \left(We\ r\right)^{-0.266}$ is Sauter Mean Diameter of drops. The deflection distance of the spray axis at each time step due to swirl is: $\Delta y = U_t\ \Delta t\ \cos b$, where: Δt is time step, b is an angle between radius and current sector of axis. Deformation by swirl of windward Δy_3 and leeward Δy_4 generating lines of the spray core cross section are calculated for each time step as:

$$dy_3 = -C_{30}\, A_{wt}\, (W_t - U_t)\ \Delta t\ \cos b\ ;$$
$$dy_4 = C_{40}\, A_{wt}\, (W_t - U_t)\, \Delta t\ \cos b \quad (21)$$

where: $C_{30} \approx 0.2$ and $C_{40} \approx 1.6$ are empirical coefficients.

After wall impingement a dense near-wall flow consisting of fuel drops and air, arises. The NWF expands on a surface in all directions. The shape of NWF spot depends on impingement angles: g_j, (j = 1, 2, 3, 4) (see Fig. 7).

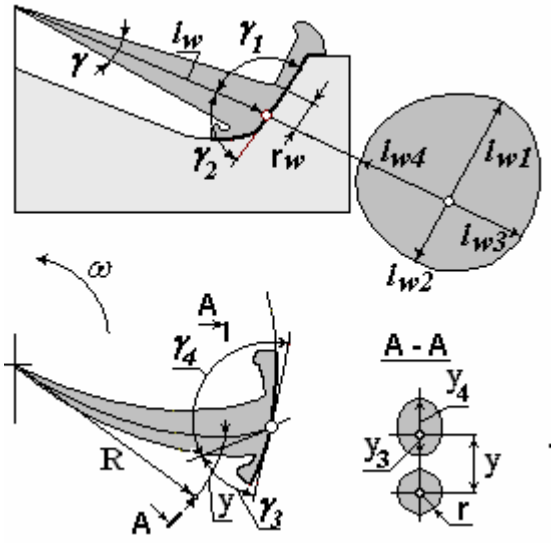

Figure. 7. Schematic of a spray and near-wall flow in swirling air.

Impingement angles are calculated with allowance for swirl transfer of a spray and the shape of a piston bowl in a place of impingement. Dimensions of NWF spot in each directions l_{wj} (j =1, 2, 3, 4) are defined as follows:

$$l_{wj} = K_j\, B_{sw}^{0.5}\, t_w^{0.5}; \qquad t_w = t_s - t_{sw}; \quad (22)$$

$$B_{sw} = \left[\left(f + 0.08\, K_{j\max}\right) / K_{j\max} \left(l_{b\max} - l_w\right)\right]^2 / \left(t_{s\max} - t_{sw}\right)$$

where: f = 0.6 is the factor of losses due to impingement, t_{sw} is the time of impingement[1], $t_{s\,max} = t_{inj}$ + (0.3÷0.5)10^{-3} [s] is the time of complete spray

[1] Actually the wall impingement starts from the moment of spray front contact with an oblique surface of the piston and is completed by full transition of fuel from the front in the core of NWF. Due to schematic description of RK-model in this paper, this algorithm is skipped here.

evolution, $l_{b\ max}$ is a free spray length in complete evolution, l_w is the distance covered by a spray before impingement.

On the basis of experimental photo-records made by Gavrilov, Koptev, and Plotnikov the following expression for NWF spot dimensions versus impingement angles γ_1, γ_2, γ_3, γ_4, (fig. 7) was derived by Gavrilov [25]:

$$K_j = \sqrt{sing_1\, sing_3} + 1.2\left(1 - sing_j\right) - 2\left(cosg_j\right)^3; \quad (23)$$

$$K_{j\,max} = MAX\left(K_1, K_2, K_3, K_4\right).$$

The time of wall impingement t_{sw} is determined by the equations (13, 14, 20) with account for spray tip 3-D coordinates and piston movement.

Comparison of calculations of the spray tip penetration and NWF borders evolution by equations (6-23) with the experiment is shown in Fig. 8. The measured values are marked with points, frame numbers correspond to those in Fig. 3. Subscript "*free*" means free spray evolution (without walls).

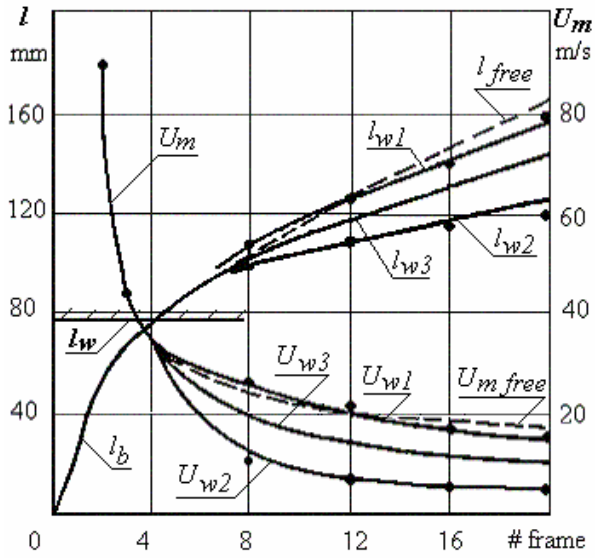

Figure. 8. Spray evolution phenomena in conditions of turbocharged diesel: S/D=300/230, RPM=750, m_f = 0.62 g. U_{wj} are velocities of corresponded NWF borders. Data was obtained by Razleytsev [6].

For visualization of fuel spray evolution a special Fuel Spray Visualization (FSV) computer code has been developed. Spray images presented below are obtained with this code. Comparison of the calculated image of spray and NWF evolution with the experimental photo-record is presented in Fig. 9. Frame “b” shows pictures of near-wall flows obtained by superposition of shooting frames with the sprays images artificially removed. The shapes of the NWF spots experimentally obtained agree with the calculated ones.

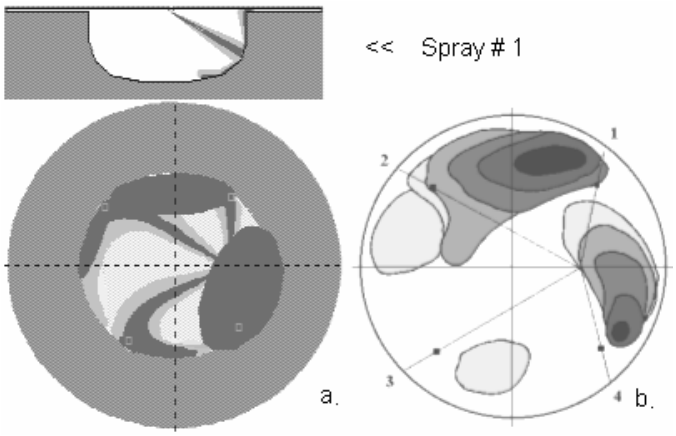

Figure 9. Comparison of calculated image of spray and NWF evolution (a) with experimental photo-record (b) of tractor diesel: S/D =140/120, RPM=1800.

DISTRIBUTION OF FUEL IN A SPRAY

The principles of simulation of fuel distribution in a spray used in the RK-model were derived by Razleystev [6]. A spray, which is injected into the combustion chamber, is divided into 7 characteristic zones as shown in Fig. 10. Each zone has own conditions of evaporation and burning and these conditions are uniform within a whole zone.

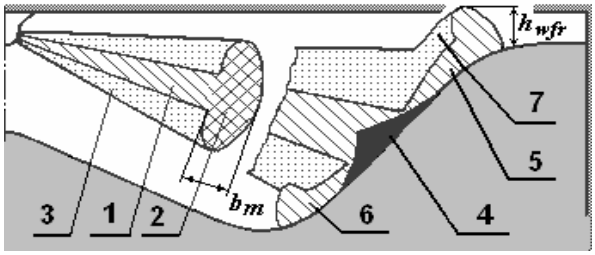

Figure 10. Characteristic zones of the diesel spray.

During the time prior to the jet impingement only three zones are considered in the spray. These are: 1 - dense conical core, 2 - dense forward front, 3 – dilute outer sleeve. The near-wall flow being formed after impingement is inhomogeneous in structure, density and temperature, which makes the calculation of fuel evaporation difficult; it is therefore expedient to distinguish typical zones with averaged heat and mass transfer coefficients in the near-wall flow by analogy with the free spray. After wall impingement, a new set of zones is taken into account: 4 - axial conical core of a NWF, 5 - dense core of a NWF on a piston bowl surface, 6 - dense forward front of a NWF, 7 - dilute outer zone of NWF. If during its evolution, the spray reaches the surface of the cylinder liner and/or the head of the cylinder then it is necessary to introduce two further zones. Depth of spray forward front is calculated as:

$$b_m = A_m\, l\, F_s\, We^{0.32} M^{-0.07}\, r^{0.5}; \quad (24)$$

where Am ≈ 0.7 is empirical coefficient. The sequence of calculation of fuel distribution in the zones at each moment t_s (varying from 0 up to $t_{s\ max}$ with some increment) is the following.

1. The fuel fraction s_s injected into the cylinder is determined from the injection profile: $s = f(t)$.
2. The spray length l at current t_s can be expressed by equations (13, 14).
3. Moment of injection of EFM braked in the front at the distance l from the nozzle can be calculated as: $t = t_s - t_m$, where t_m is defined from equation (3).
4. The fuel fraction s_t injected into the cylinder at time t is determined from the injection profile: $s = f(t)$.
5. The distance between the nozzle and a section behind spray front is $l_k = l - b_m$. See Fig. 10 and equation (24).
6. Time of injection of EFM achieved the section behind spray front t_k is calculated by equations (3, 5, 13, 14).
7. The fuel fraction s_k injected into the cylinder at time t_k is determined from the injection profile: $s = f(t)$.

Distribution of fuel among the spray zones is defined for each time step by following expressions:

in core: $$s_{core} = (s_s - s_k)(1 - 0.1 l_k / l); \quad (25)$$

in front: $$s_{front} = 0.8\ (s_k - s_t) A; \quad (26)$$

in dilute outer sleeve:

$$s_{env} = s_t + 0.2(s_k - s_t) + (s_s - s_k)\, 0.1\, l_k / l; \quad (27)$$

in NWF: $$s_W = 0.8\ (s_k - s_t)(1 - A); \quad (28)$$

where: A = 1 before wall impingement, and A=0 after.

After spray and wall impingement an additional control section $l_k = l_w$ is introduced to define fuel fractions allocated in the zones of NWF: outer sleeve $s_{w\,env}$, core $s_{w\,core}$ and front $s_{w\,fr}$; and the calculation is continued according to the similar plan. If NWF spot achieves the piston crown, a fuel fraction in this zone s_{crown} is defined by relation:

$$s_{crown} = s_W\, V_{crown} / V_W. \quad (29)$$

If NWF forward front reaches the cylinder head surface as shown in Fig. 10, a fuel fraction in the cylinder head zone s_{head} is defined by relation:

$$s_{head} = s_{w\,fr}\, V_{head} / V_{w\,fr}; \quad s_{w\,fr} = s_{w\,fr} - s_{head}. \quad (30)$$

The condition of the fuel-air mixture allocation on the cylinder head surface is described by expression:

$$h_{w\,fr} = F_{sw}\, l_{w1}\, We^{0.32} M^{-0.07}\, r^{0.5} > h_{clr}, \quad (31)$$

where: $h_{w\,fr}$ is the height of NWF forward front (see Fig. 10), h_{clr} is the piston-head clearance depended on CA, $F_{sw} \approx 1.5\, F_s$.

If NWF spot reaches the cylinder liner, a fuel fraction in the liner zone s_{liner} is defined by relations:

$$s_{liner} = s_W\, V_{liner} / V_W;\ C_{liner} = 1 - V_{liner} / V_W. \quad (32)$$

Remaining fuel fractions in the zones of NWF are:

$$\begin{aligned} s_{w\,core} &= s_{w\,core}\, C_{liner}; \\ s_{w\,fr} &= s_{w\,fr}\, C_{liner}; \quad s_{w\,env} = s_{w\,env}\, C_{liner}; \\ s_W &= s_{w\,core} + s_{w\,fr} + s_{w\,env}. \end{aligned} \quad (33)$$

If two adjacent near-wall flows intersect, the fuel fraction in the intersection zone s_{cross} is defined by the expression:

$$s_{cross} = V_{cross} / V_W\ \left(s_{w\,core} + s_{w\,fr} + A_{w\,env}\ s_{w\,env}\right); \quad (34)$$

where $A_{w\_env} \approx 0.5$ is the coefficient taking into account a decrease in NWF environment formation due to NWF spots intersection. Remaining fuel fractions in the zones of NWF are:

$$\begin{aligned} s_{w\,core} &= s_{w\,core}\,(1 - V_{cross} / V_W); \\ s_{w\,fr} &= s_{w\,fr}\,(1 - V_{cross} / V_W); \\ s_{w\,env} &= s_{w\,env}\,(1 - A_{w\,env} V_{cross} / V_W). \end{aligned} \quad (35)$$

Overall fuel fraction in the NWF of one spray is:

$$s_W = s_{w\,core} + s_{w\,fr} + s_{w\,env}.$$

Volumes of characteristic zones: V_W, V_{crown}, V_{head}, $V_{w\,fr}$, V_{liner}, V_{cross} in equations (29 – 35) are calculated as volumes of spatial geometrical figures crossed by planes or other figures. Because the intention of this paper is to explain only the general scheme of the RK-model, bulky expressions defining the volumes of zones on surfaces of piston, liner and the cylinder head are skipped.

The order of calculation is as follows:

1. Every spray is simulated on the assumption that the spray is alone.
2. The fuel fractions are summed in each zone for all sprays.

Results of calculations of fuel distribution in the zones for different diesels are presented in Fig. 11, 12. All calculations were carried out with identical sets of calibration constants.

If the sprayer is not central or spray angles are not identical, as it shown in Fig. 11, every spray is simulated independently with its own conditions of swirl effect as well as times and angles of wall impingement. Frame *a* in Fig.11 corresponding to CA=362^0, presents different phases of sprays and wall impingement. The period from the beginning of first spray impingement until the end of last spray impingement is 5 CA deg. (from 360^0 up to 365^0). Curves in Fig. 11 present sum of fuel fractions for all seven sprays. In a compact combustion chamber of a heavy-duty truck diesel there is not space enough for free evolution of near-wall flows. Intersections of some near-wall flows begin already in the middle of injection,

see frame *b*. A sensible rise in the fuel fraction in the zones of NWF intersection takes place at the end of injection, see Fig. 11, curve s_{cross} and frame *c*. Due to this negative effect, the amount of fuel in the zone of dilute outer sleeve becomes less (see curve: $s_{env}+s_{wfr}+s_{wenv}$ in Fig. 11) and combustion rate decreases.

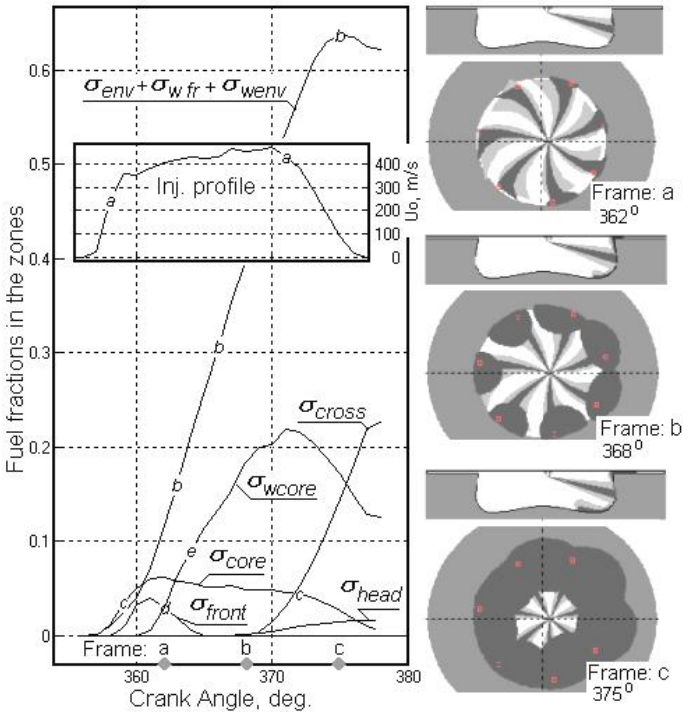

Figure. 11. Results of simulation of fuel allocation in the characteristic zones in combustion chamber of truck diesel: S/D=140/130, RPM=1700.

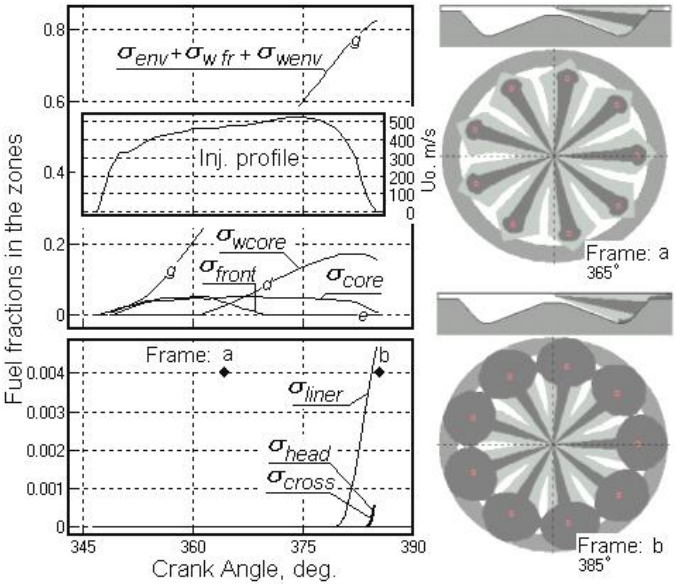

Figure. 12. Results of simulation of fuel allocation in the characteristic zones in combustion chamber of medium speed diesel: S/D=260/260, spray angle 160^0, RPM=1000, BMEP=15 bar.

If the sprayer is central and spray angles are identical, as it shown in Fig. 12, only one spray is simulated. Afterwards the results obtained are summarized. Usually in medium-speed diesel with Hesselman combustion chamber, sprays have more space for free evolution, therefore more fuel is distributed in the zones with good evaporation conditions: dilute outer sleeve and forward front. Curve: $s_{env}+s_{wfr}+s_{wenv}$ in Fig. 12 shows that fuel fraction in these zones exceeds 80%, whereas, in diesels with compact combustion chamber this fraction usually lies in the range 60…70%. Due to the acute angle of spray and wall meeting, NWF expands intensely in radial direction and can reach the cylinder liner surface, see frame: *b* and curve s_{liner} in Fig. 12. The liner zone has bad evaporation conditions, and it is essential to exclude hit of fuel in this zone. This is especially important for engines with a very shallow piston bowl. Example in Fig. 12 shows very small fuel fractions distributed in the NWF crossing zone, in the liner zone and cylinder head zone, because the injected fuel mass is not large.

FUEL EVAPORATION MODELING

During injection and evolution of sprays the rate of combustion is limited mainly by the rate of fuel evaporation. The zones of intensive heat exchange and evaporation of injected fuel exist in the free spray. These are forward front and dilute outer sleeve of a spray. In a high-speed and dense axial flow core the heating is low and evaporation of drops is insignificant. At wall impingement, the evaporation rate of fuel accumulated in forward front is reduced sharply to a minimum at the moment of the end of front stacking on a wall (zone 4 in Fig. 10). It is caused by the lower (in comparison with gas) temperature of a wall, reduction of blow of drops, condensation of drops and gas mixture on a wall, merge and interfusion of vanguard drops with colder drops flying up to a wall. After front impingement with a wall, the two-phase mixture begins to spread on a wall outside the borders of cone 4 (Fig. 10) of a spray. The evaporation rate of fuel in the wall surface zone is increased, though remains smaller than in the chamber volume. To facilitate simulation there, simplified assumptions are adopted:

1) During injection the intensive heat exchange and evaporation take place in the zones of dilute outer sleeve, forward front and NWF. Evaporation in the zone of spray core is neglected.

2) The evaporation rate of fuel in each zone of intensive heat exchange is equal to a sum of evaporation rates of separate drops. The evaporation of each drop before and after ignition of fuel is simulated by the Sreznevsky's equation:

$$d_k^2 = d_0^2 - K\, t_u\,; \qquad (36)$$

where: d_k is the current diameter of drop; d_0 is the initial diameter of drop; K is the constant of evaporation; t_u is the current time from evaporation beginning (from arrival of the drop in the zone).

3) The fuel equipment of supercharged diesels provides rather uniform atomization of fuel, especially at the basic phase of injection. Therefore, the calculation of evaporation of fuel can be carried out on a base of a mean Sauter drop diameter d_{32}. It is assumed: $d_0 = d_{32}$.

4) The relation $K/d_0^2 = b_u$ in each zone is a constant during injection period.

5) Neglected factors and inaccuracies of adopted assumptions will be corrected by empirical correction function Y, see equation (41) below.

Equation of related fuel evaporation rate ds_{ui}/dt was obtained by Razleytsev [6] for i-zone from the noted assumptions:

$$ds_{ui}/dt = \left[1-\left(1-b_{ui}t_{ui}\right)^{3/2}\right] s_{zi}/t_{ui}\,; \qquad (37)$$

$$t_{ui} = t_s - t_{s0i} \qquad (38)$$

where: t_{s0i} is the time of distribution of fuel in i–zone; s_{zi} is the fuel fraction in the i–zone. Constants of evaporation of fuel in various zones are determined from the equation:

$$K_{ui} = 4\cdot 10^6\, Nu_D\, D_p\, p_S / r_f \qquad (39)$$

where: Nu_D is the Nusselt number for diffusion process; D_p is the diffusion factor for fuel vapor under combustion chamber conditions; p_S is the pressure of saturated fuel vapor; r_f is the density of liquid fuel. The diffusion factor is calculated from the following expression:

$$D_p = D_{po}\left(T_k/T_o\right)\left(p_o/p\right) \qquad (40)$$

where: D_{po} is the diffusion factor under atmospheric conditions [p_o, T_o], T_k is the equilibrium temperature of evaporation, p is the current pressure in the cylinder. Different conditions of evaporation in zones of spray are taken into account by corresponding settings of T_k and Nu_D.

In the dilute outer zones there is a large distance between fuel drops and there is small decrease of temperature caused by evaporation. Therefore, in this zone it is assumed that Nu_D = 2 [6]. During injection and combustion, the cylinder pressure and temperature exceed critical parameters of liquid phase conversion into a gaseous one. Therefore, in this zone the evaporation constant is $K_{env}=1.12\ 10^{-6}/p$, where p is in MPa. For the case of PCCI the equations (39, 40) are used.

In the forward front zone, the cold drops from the core are rapidly heated, therefore in this zone the $Nu_D \approx 20$ [6] and temperature lies between critical (710 K) and fuel temperatures. Thus in this zone the evaporation constant is $K_{fr}=0.63\ 10^{-6}/p$. For the case of PCCI the equations (39, 40) are used.

In the zones of NWF, including zones on the cylinder head and liner walls, the evaporation constants are calculated by equations (39, 40); where T_k is some effective temperature depending on the corresponding wall temperature T_{wi}:

$$T_k = \begin{Bmatrix} 550 & if & T_{wi} \le 400 \\ a\,T_{wi}^3 + b\,T_{wi}^2 + c\,T_{wi} + d & if & 400 < T_{wi} < 700 \\ 700 & if & 700 \le T_{wi} \end{Bmatrix};$$

where: a = 0.000000243; b = 0.001017919;
c = -0.854312919; d = 709.55496.

The Nusselt number for NWF in equation (39) depends on the surface shape: for smooth surface of the combustion chamber: Nu_D = 2; for shaped surfaces, making turbulent flow: Nu_D = 3 or higher [6]. A 15-year experience of the RK-model calibration for different types of engines with cylinder diameter from 75 mm up to 760 mm, with different combustion chambers and injector designs, working over the whole operating range, allows the empirical correction function Y depending on a swirl ratio, engine speed, piston stroke and Sauter mean diameter to be proposed in the form:

$$Y = 0.372\cdot 10^{-9}\left(18 + y_S + y_{RPM}\right) y\, R_{Sy}^{0.35}\, d_{32}^{-1.5}\,; \qquad (41)$$

where: $y_S=f(S)$ is the correction factor depending on piston stroke S, $y_{RPM}=f(RPM)$ is the correction factor taking into account engine speed, $R_{Sy}=MAX(0.1, R_s)$ is the corrected swirl ratio in combustion chamber at TDC, $y \approx 35$ is the factor for RK-model calibration. Factor y does not depend on the engine load and speed and is designed for accurate RK-model calibration. As a rule, essential calibration is not required. Considering the correction factor, the evaporation constant for i-zone is: $b_{ui} = Y\,K_i/d_{32}^2$. Fuel evaporation rate in each zone is calculated by equation (37). Overall evaporation rate is a sum of evaporation rates in all m zones:

$$\frac{ds_u}{dt} = \sum_{i=1}^{m} ds_{ui}/dt\ . \qquad (42)$$

In the case of multiple injection the simulation of spray evolution, distribution of fuel in the zones and evaporation of fuel is carried out for each portion of split injection. The characteristic gas temperature and pressure for each portion are taken from previous cycle simulation.

HEAT RELEASE SIMULATION

The assumption is made that the heat release process consists of four main phases. They differ by physical and chemical peculiarities and factors limiting the rate of the process:

1. Induction period. In the case of long induction period at PCCI the low temperature oxidation is possible.

2. Premixed combustion phase.
3. Mixing-controlled combustion phase.
4. Late combustion phase after the end of fuel injection.

When modeling the engine with multiple injection, the combustion of every injected portion is simulated separately taking into account the values of injected fuel mass and air-fuel ratio for each portion.

PREDICTION OF AUTO-IGNITION DELAY PERIOD FOR HIGH TEMPERATURE COMBUSTION

The auto-ignition delay period has to be predicted for each fuel portion during multiple injection. Fuel of second (j =2), third (j =3) and later (j =4, 5, etc.) portions can be injected after TDC with great delay and into a surrounding with a large burnt gas fraction. These specific conditions make the use of classic formulas for calculation of the auto-ignition delay period incorrect. The equation providing a good agreement between simulation results and measurements for various type engines was derived in the present work on the basis of experimental data processing.

The auto-ignition delay period t_i for each j-portion was calculated by different ways for different engines working on different operating conditions. The obtained results were compared.

1. Step-by-step calculation from Start Of Injection (SOI) until the Start Of Combustion (SOC) being calculated as

$$SOC = \Theta - SOI + t_{iT}\left(p(\Theta), T(\Theta)\right)\cdot 6\,n \quad ; \qquad (43)$$

$$t_i = SOC - SOI$$

where: Θ in deg. is the crank angle varying by small time step $\Delta\Theta$ from SOI up to the moment where calculated SOC begins to rise; p and T are current cylinder pressure in MPa and temperature in K (both ones are the functions of crank angle Θ); n is the engine speed [RPM]; t_{iT} in sec. is ignition delay determined from the modified Tolstov's [38] expression:

$$t_{iT} = 3.8\cdot 10^{-6}\left(1-1.6\cdot 10^{-4} n\right)\left(\frac{T}{p}\right)^{m}\exp\left(\frac{E_a}{8.312\,T}\right)C_C C_T \quad ; (44)$$

C_T is the correction factor accounting for temperature growth rate during auto-ignition delay period; C_C is the correction factor accounting for the concentration of combustion products taking place during delay period; *m=MAX(0.5, (0.64 – 0.035 p))* is exponent depending on current cylinder pressure; E_a = 23000...28000 kJ/kmole is the apparent activation energy for the auto-ignition process. The expression for exponent m was implemented to account conditions of small cylinder pressure at very early injection. In the original Tolstov equation [38] C_C =1 and C_T =1 (not used), the m = 0.5 and is a constant, as well another factors are balanced for usage the boost air pressure and temperature. Also the original equation was derived and is working well for the conditions of conventional fuel injection with SOI = 5…20 deg. before TDC and at small residual gas fraction. So, to account condition in the new engines with PCCI, large EGR and multiple injection, the additional factors were implemented into Tolstov expression.

Factor C_T takes into account a gradient of the temperature during delay period which may be negative at the start of injection after TDC. Late injection results in increase the delay period. The correction factor C_T was derived by the experimental data processing. The experimental data for the Caterpillar (D/S = 137/165 mm) diesel were published by Bakenhus and Reitz [39]; the data for the D49 (D/S = 260/260 mm) locomotive diesel with double injection were presented by Kolomna plant. Factor C_T is determined as:

$$C_T = 1, \qquad if\ x_t > 30;$$

$$C_T = -4\cdot 10^{-7} x_t^3 + 5\cdot 10^{-5} x_t^2 - 0.0032\,x_t + 1.0832,\ if\ x_t < 30;$$

$$x_t = \frac{T(\Theta) - T(\Theta - \Delta\Theta)}{1000\,\Delta\Theta} 6n;$$

where: $T(\Theta)$ and $T(\Theta–\Delta\Theta)$, in K are mean cylinder temperatures at the current time moment and at the previous time moment. Dependence $C_T = f(x_t)$ is given in Fig. 13.

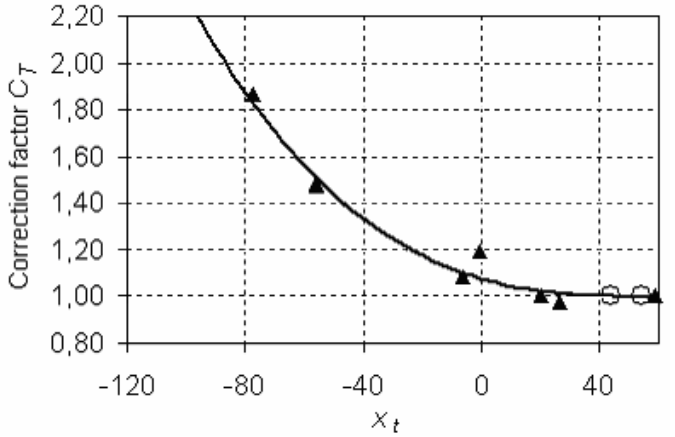

Figure 13. Correction factor C_T accounting for temperature growth rate x_t in the auto-ignition delay period. Symbols:
▲ - Bakenhus and Reitz data [39];
O – Kolomna plant data.

The correction factor C_C accounting composition of air charge was derived by the experimental data processing. The experimental data published in [39, 40, 41] were obtained for engine conditions and bomb. Fig. 14 shows the correction factor C_C versus composition of gas wherein fuel has been injected, as well as the approximation curve marked by bold line.

Both correction factors are equal to 1 for a conventional diesel with small injection timing. However, the farther is injection from TDC, the greater the correction factors will be. During multiple injection when the succeeding portions are injected into the surrounding with developed combustion and increased temperature, the correction

factor C_T is near to 1 and the correction factor C_C has a decisive effect on the calculated auto-ignition delay of the next fuel portion.

Results of ignition delay simulation with presented technique in comparison with published experimental data are shown in the Fig. 15 and marked by symbol □. The calculated delays at large SOI exceed the experimental data. List of engines and their operating modes being used for plotting the diagram of Fig. 15 is presented in the table below.

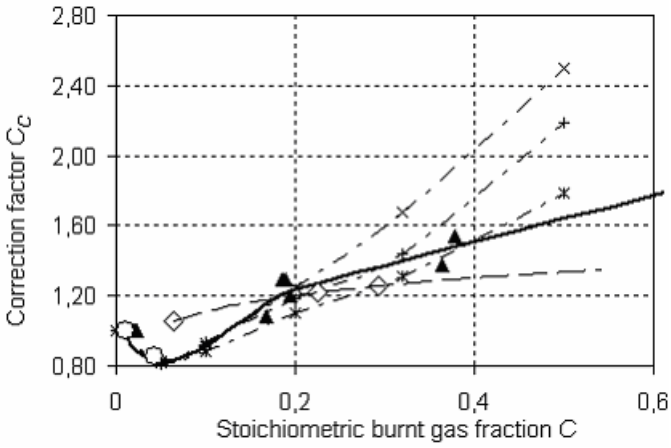

Figure 14. Correction factor C_C accounting for stoichiometric burnt gas fraction during the autoignition delay period. Symbols:
▲ - Bakenhus and Reitz [39];
◊ - Schneider, Stockli, Lutz, Eberle [41];
O – Kolomna plant;
data for the bomb were obtained by Kwon, Arai, Hiroyasu [40] at temperatures:
Ú) T=700K, x) T=773 K, +) T=823K.

Engine	D/S [mm]	RPM	BMEP [bar]	Source
DKRN 74/160	760/1600	120	9.5	*
VASA 6R46	460/580	500	22.7	[45]
		400	13.9	
		315	9.5	
D42	300/380	750	16	*
D49	260/260	1000	15.7	*
		845	11	
		563	3.3	
Cold start at -25C		350	0.16	
Experimental DI, PCCI	135/140	1000	0…2.4	[42, 43, 44]
KamAZ 7405	120/120	2200	12.2	*
		1800	13.8	
		1000	12	

* Data were presented by the engine manufacturer.

Analysis of the data shows the calculated values of ignition delay exceed the measured ones.

2. Integral calculation [16] proposes the calculation of the t_i by integration of the relation:

$$\int_0^{t_i} \frac{dt}{t_{iT}} = 1 \qquad (45)$$

where t_{iT} is calculated by equation (44). The results obtained with this kind of calculation are shown in the fig. 15 by symbol Δ. They are less than the measured data at large SOI.

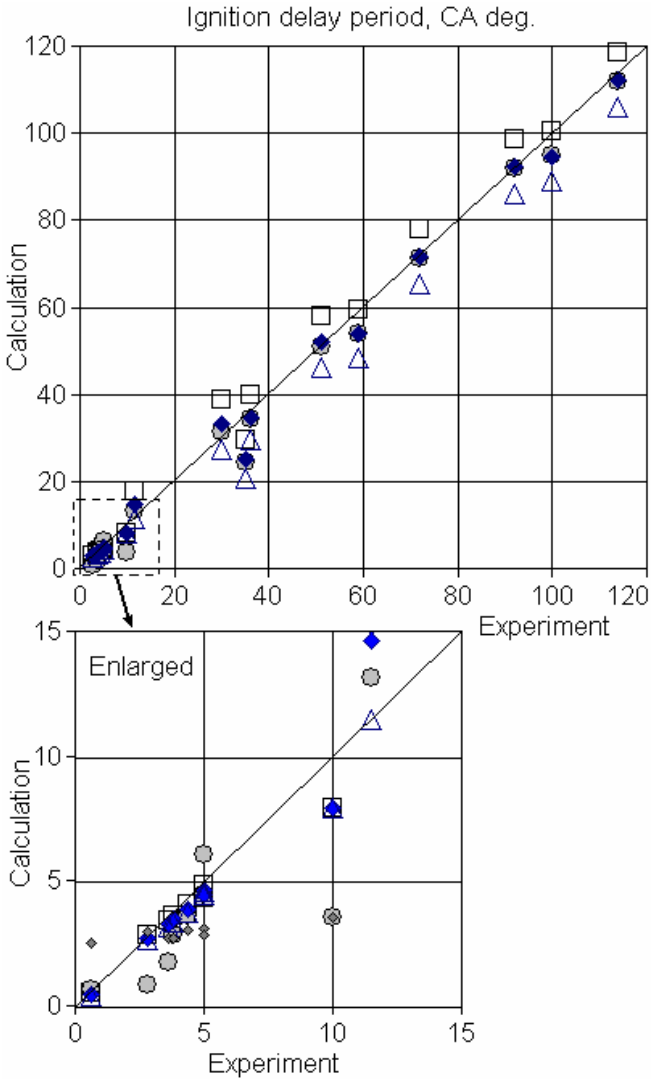

Figure 15. The comparison of the experimental ignition delays for different engines with calculated by different methods. Symbols:
□ – Step-by-step calculation with eq. (43, 44);
Δ – Integral calculation with eq. (45, 44);
♦ – Average calculation with eq. (43, 44, 45);
● – Expression of Michigan University [46];
♦ – Calculation with Hardenberg and Hase expression [47].

3. Average calculation uses arithmetic mean of the both previous values. The obtained data are marked by symbol ♦ in the Fig. 15. They have very good agreement with the experiments over the whole range of delay varying.

4. Expression of University of Michigan [46] proposes the calculation of the t_i by integration of the relation:

$$\int_0^{t_i} \frac{dt}{t_{ign}} = 1; \quad t_{ign} = 1.3\cdot 10^{-4}\, p^{-1.05} f^{-0.77} y_{O2}^{-1.41} \exp\left(\frac{33700}{RT}\right). \tag{46}$$

where: f is air fuel ratio, y_{O2} is a concentration of oxygen, T and p are current cylinder temperature in K and pressure in atm. The obtained data are marked by symbol ● in the Fig. 15.

5. Hardenberg and Hase expression [47] can not be used at PCCI because one is bounded by the range with high cylinder pressure. The obtained data are marked by small symbol ♦ in the Fig. 15.

Analysis of data presented in the Fig. 15 allows recommend for engines with PCCI the Average calculation (# 3) or expression of University of Michigan (# 4) as providing the most accuracy. Average calculation (# 3) is preferable at conventional conditions where ignition delay is less 10 CA deg. and for engines with SOI after TDC.

PREDICTION OF AUTO-IGNITION DELAY PERIOD FOR LOW TEMPERATURE COMBUSTION

The Low Temperature Combustion (LTC) precedes the High Temperature Combustion (HTC). Now days for simulation of the LTC and HTC as well for prediction the ignition delays for them the CHEMKIN code is mainly used. Some authors note the LTC combustion starts in the narrow range of the in-cylinder temperature: from 770 up to 810 K. But it does not allow prediction of the LTC start with necessary accuracy. In the presented research there was made attempt to predict the LTC ignition delay on the base of HTC ignition delay being computed before. Analysis of numerous published experimental and calculated data [42-44, 48-51] allows derive the easy expression for LTC delay t_{iLTC} as function of HTC delay t_{iHTC} and EGR ratio. Fig. 16 shows the dependence of difference between HTC delay and LTC delay versus HTC delay for different engines working at different RPM, BMEP, temperatures of intake air, etc. Processing of the

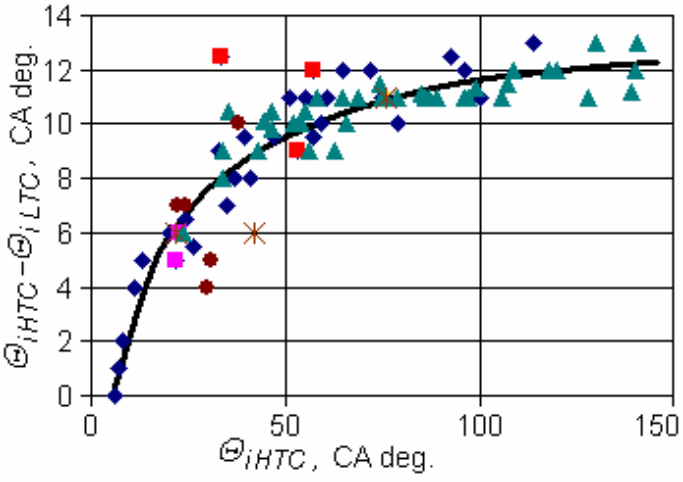

Figure 16. Difference between HTC delay and LTC delay versus HTC delay period.

presented data allows recommend the expression for LTC delay prediction:

$$\Theta_{iLTC} = 8.281 + 1.0259\,\Theta_{iHTC} - 4.8822 \ln \Theta_{iHTC} - \sqrt{31.602\, C} \tag{47}$$

where: $\Theta_{iLTC} = t_{iLTC}\, 6n$; $\Theta_{iHTC} = t_{iHTC}\, 6n$ are the LTC delay and HTC delay in CA degrees; C is EGR fraction.

HEAT RELEASE PREDICTION FOR LTC

Fraction of fuel burning by low temperature mechanism can be calculated with expression derived by processing the same published data [42-44, 48-51]:

$$x_{LTC}^{\max} = (0.102 - 0.0392\, C)\cdot\left(\frac{81.6}{\exp\Theta} - \frac{8.88}{\Theta} + 1.2261\right) \tag{48}$$

where Θ = *MAX (6.7, Q_{iLTC})*.

Heat release of LTC can be approximated with Wiebe expression, as a function of crank angle j varied from the beginning of LTC:

$$x_{LTC}(j) = x_{LTC}^{\max}\left\{1 - \exp\left[-2.9957\left(\frac{j}{j_z}\right)^{m_v+1}\right]\right\} \tag{49}$$

where: m_v = *1.2+0.69 C* is a mode of Wiebe function; j_z = 6…8 CA deg is a duration of the LTC.

HTC HEAT RELEASE PREDICTION

Fraction of fuel burning at HTC is $x_{HTC}^{\max} = 1 - x_{LTC}^{\max}$.

Detailed description of equations obtained by Razleytsev for heat release calculation is presented in [6]. During premixed combustion phase the heat release rate is:

$$dx/dt = f_0 P_0 + f_1 P_1 \tag{50}$$

where: $P_0 = A_0 (m_f/V_i)(s_{ud} - x_0)(0.1 s_{ud} + x_0)$;
$P_1 = ds_u/dt$.

During mixing-controlled combustion phase, heat release rate is:

$$dx/dt = f_1 P_1 + f_2 P_2 \tag{51}$$

where $P_2 = A_2 (m_f/V_c)(s_u - x)(a - x)$.

After fuel injection, at late combustion phase the heat release rate is:

$$dx/dt = f_3 A_3 K_T (1-x)(x_b a - x). \tag{52}$$

In these equations it is assumed that $f_0 \approx f_1 \approx f_2 = f$ is the function describing completeness of fuel vapor combustion in the zones:

$$f = 1 - \frac{A_1}{x_b a - x}\left\{r_V + \sum_{i=1}^{m_W}\left[300\, r_{Wi} \exp\left(\frac{-16000}{2500 + T_{Wi}}\right)\right]\right\}\frac{dx}{dt} \tag{53}$$

where: x_b is the efficiency of air use, α is the equivalence A/F ratio, r_V is the relative evaporation rate in the zones of outer sleeve and front, r_{Wi} is relative evaporation rate in different NWF zones:

$$r_V = \frac{ds_{u\,env}/dt \; + \; ds_{u\,front}/dt}{ds_u/dt}, \quad r_{Wi} = \frac{ds_{u\,Wi}/dt}{ds_u/dt},$$

m_W is the current number of zones formed by NWF, T_{Wi} is the wall temperature of a corresponding zone. The efficiency of air use is described by the relation of current equivalence A/F ratio in zones of combustion to overall A/F ratio in the cylinder defined as a. On the basis of gas analysis testing for different diesel engines, the expression for x_b was obtained by Razleytsev in the form:

$$x_b = 1 - 1.46\,(1 - x_{b0})\frac{\bar{j}_z}{\bar{j}_{z0}}\frac{2}{p}\exp\left[-\frac{1}{2}\left(\frac{\bar{j}_z}{\bar{j}_{z0}}\right)^2\right] \qquad (54)$$

where: $\bar{j}_{z0}$=0.25...0.35 is a constant, $\bar{j}_z = j/j_z$ is the current CA from combustion beginning (j) related to conventional combustion duration j_z, x_{b0} =0.35...0.45 for diesels with compact piston bowl, and x_{b0} =0.20...0.35 for medium and high speed diesels with open combustion chamber (Hesselman). The conventional combustion duration is determined by the evaporation period of large drops injected at the end of injection:

$$j_z = (t_{inj} - t_i + t_{l\,burn})\,6n; \qquad (55)$$

$$t_{i\,burn} = d_l^2/K_u\left[1 + 2.5\cdot 10^6\; K_O/(a-1)\right];\; K_u = Y\,K_O;$$

where d_l is the largest drop diameter. In equations (50-55) the following notations are used: m_f is the fuel mass injected into the cylinder at current portion and before (in previous portions), V_i and V_c are cylinder volumes at beginning of HTC of current fuel portion and at TDC, s_{ud} and s_u are fuel fractions evaporated during ignition delay period up to the current moment, respectively, A_0, A_1, A_2 are empirical factors depending on engine speed and swirl intensity, A_3 can be found from equations (51, 52) at $t = t_{s\,max}$. The experience of RK-model calibration for different engines allows recommendation of the following:

$$A_0 = a_0\,(R_S\,n)^{0.5};\; A_1 = 0.04/(R_S\,n)^{0.5};\; A_2 = 9\,(R_S\,n)^{0.5}. \qquad (56)$$

K_T takes into account the destruction of NWF on a piston crown due to piston acceleration and is connected with a phenomenon in narrow clearance between the piston and the cylinder head:

$$K_T = \begin{cases} 1, & if\;\; Z < Z_n \\ 1 + 3000\,s_{crown}\left(Z^2 - Z_n^2\right), & if\;\; Z \ge Z_n \end{cases};$$

$$Z = (dV/dj)/V$$

where: V is the current cylinder volume, j is the CA, Z_n is Z at 15° after TDC. The presented combustion model allows prediction of heat release in the cylinder without recalibration for each operating mode. Fig. 17 shows the calculated cylinder pressure and heat release curves in comparison with experimental data for truck V-diesel (S/D=120/120, with traditional mechanical fuel injection system) operating over the external performance.

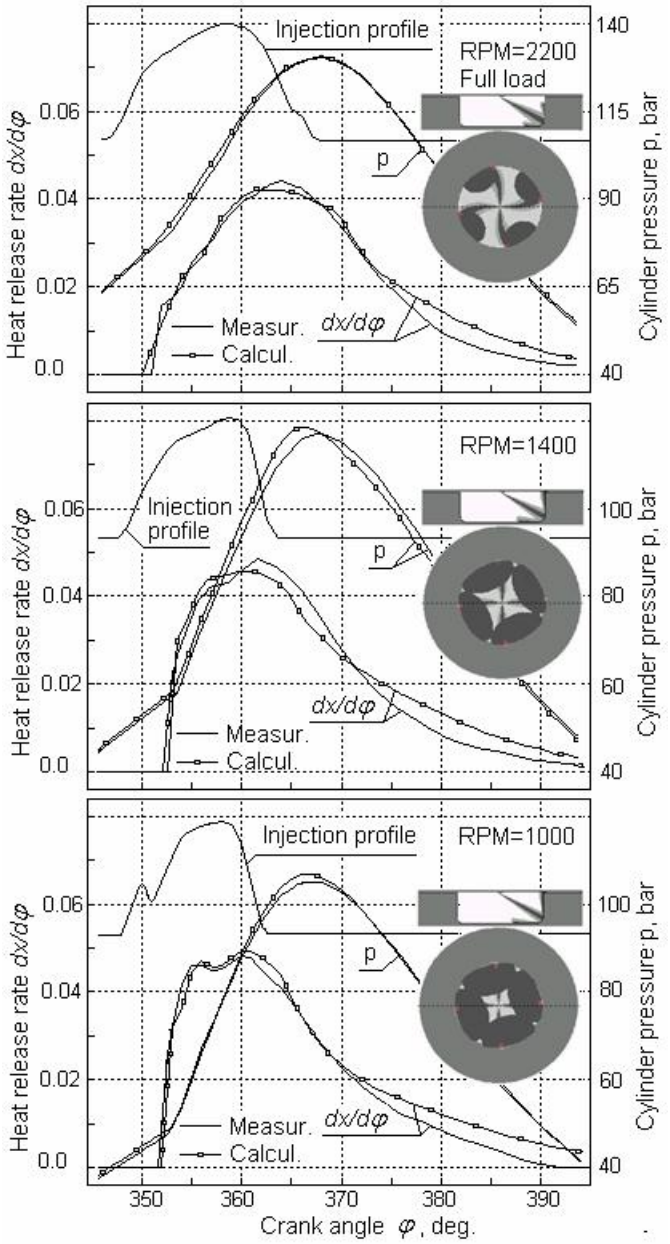

Figure 17. Cylinder pressure and heat release rate calculated curves in comparison with experimental data of truck V-diesel (S/D=120/120) operating over external performance.

RPM	m_f, g	P $_{inj\,max}$, bar	t_{inj}, sec
2200	0.0787	672	1.61 10^{-3}
1400	0.0838	530	1.82 10^{-3}
1000	0.0818	352	2.34 10^{-3}

Frames correspond to the end of injection. All results are obtained with identical values of all empirical factors of the RK-model. Measured data were obtained by JSC "KamAZ" (Russia). Fuel injection parameters are presented in the table. As it is shown in the table, fuel supplies (m_f) in all operating modes are approximately equal, but injection duration t_{inj} is higher at partial load. Therefore sprays at partial load (on external curve) have more time for evolution in more dilute conditions, therefore NWF occupies a larger area (see frames in Fig. 17).

The RK-model was implemented into a full-cycle thermodynamic engine simulation software DIESEL-RK disclosed in [52]. The software requires conventional PC, with Windows XP/Vista. Calculation time depends on the number of differently orientated sprayer nozzles and strategy of multiple injection, and usually is less than one minute including all iterations.

RESULTS OF HEAT RELEASE SIMULATION FOR ENGINE WITH PCCI

The validation of presented diesel combustion model was made to confirm the ability of the RK-model to simulate with sufficient accuracy the conventional diesel operation over whole operating range [53], to simulate diesel combustion and NO emission formation at multiple injection [1] as well to simulate diesel combustion at PCCI. The ability of the combustion model to simulate with acceptable accuracy the operation of an engine with conventional single injection, with multiple injection and EGR as well with PCCI is one of the main aims staying before combustion model developer. A generality of computer code is necessary to perform a computer optimization of the engine control algorithm at any operating mode. The computer optimization is necessary to reduce the large labor expenditures at the engine research, caused by considerable number of controlling parameters which may be used to reduce emissions and SFC simultaneously. There are few possibilities to search optimal solution: the internal DIESEL-RK library of non-linear optimization procedures [2] as well external software, for example IOSO code [54]. To co-work with an external code the DIESEL-RK has special interface using text files for data exchange.

Fig. 18, 19 show the results of mixture formation and combustion simulation in Peugeot DW10-ATED4 diesel (4L, S/D=85/88 mm) with Common Rail injection system.

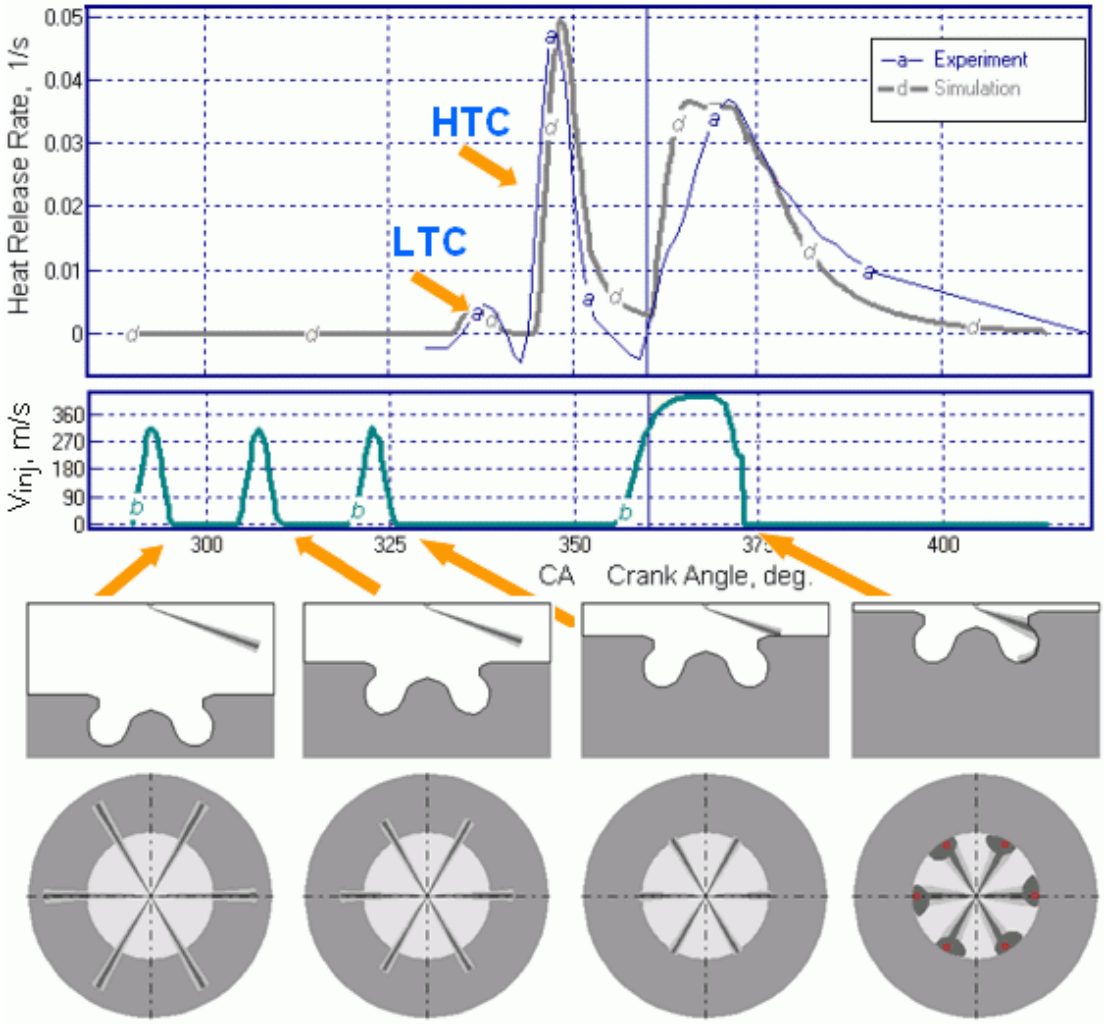

Figure 18. Results of mixture formation and combustion simulation in Peugeot DW10-ATED4 diesel. Total pilots injection fraction is 0.35.

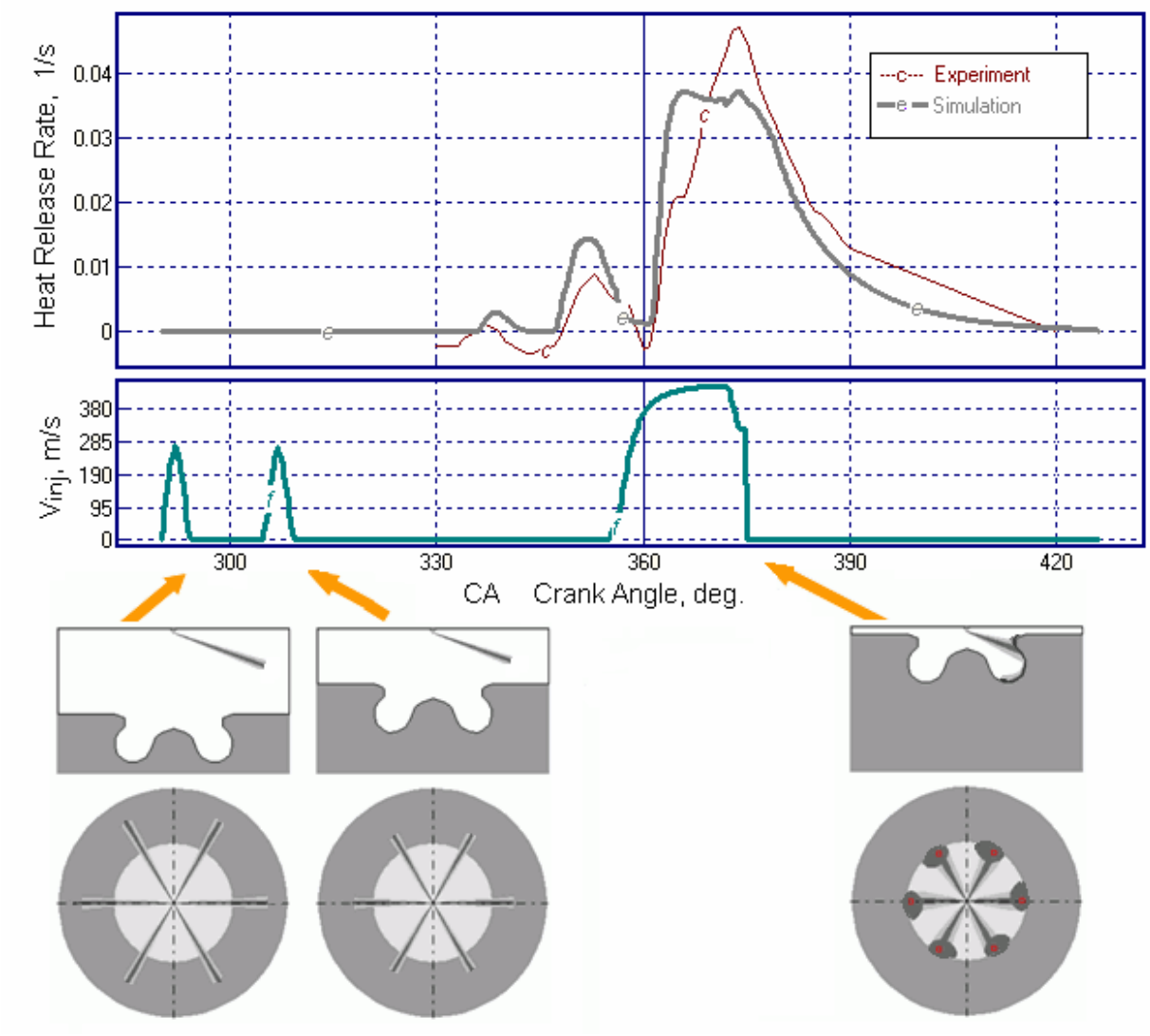

Figure 19. Results of mixture formation and combustion simulation in Peugeot DW10-ATED4 diesel. Total pilots injection fraction is 0.15.

The experimental data were obtained and published in [48]. In both cases the EGR is 9.8%. Total pilot injection fractions are 0.35 and 0.15 in the fig. 18 and 19 respectively. In both cases the PCCI was arranged by multiple pilot injections with injection timing 70 deg. before TDC. Duration of every pilot injection was so short to prevent the hitting of fuel on the cylinder liner. The injection profiles in the figures 18, 19 as well experimental heat release curves were taken from the publication [48]. Frames below diagrams show the position of sprays at the end of every injected portion. The first heat release peaks are the LTC taking place before the HTC.

SIMULATION OF NO EMISSION WITH DETAIL KINETIC MECHANISM

The presented RK-model was used for simulation of a heavy duty diesel engine with high EGR, high boost pressure and double injection. The engine data are presented in the table.

ENGINE DATA

Compression ratio	17.6
Injector	6 x 0.235
Injection pressure, bar	1700
Fuel fraction in the pilot injection	0.08
Separation after pilot injection, CA deg.	3
Injection timing, CA deg. BTDC	13.6
RPM	1800
Boost pressure, bar	3.63
EGR ratio	0.313
A/F equivalence ratio	1.49
Maximum cylinder pressure, bar	190
SFC, g/kW h	220
NOx, g/kWh	0.8

The presented combination of the engine data is character for engines with small NOx emission and specific fuel consumption. In the fig. 20 there are shown injection profile V_{inj}, Heat Release Rate curve and NOx release curves at simulation of the Nitrogen Oxides formation by Zeldovich's scheme [4, 5] and by Detail Kinetic Mechanism [5, 7, 8, 9].

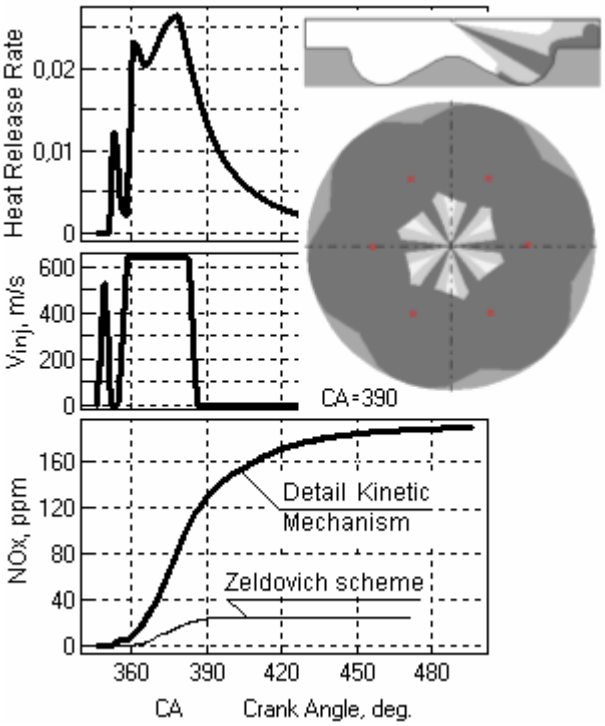

Figure 20. Injection profile V_{inj} , Heat Release Rate and NOx release curves at simulation the Nitrogen Oxides formation by Zeldovich's scheme and by Detail Kinetic Mechanism.

Presented calculated data confirm necessity to use DKM for NOx simulation at high EGR and multiple injection, because the simulation by Zeldovich's scheme does not account the formation of the prompt NO and shows too small emission level. Use the Zeldovich's scheme is correct only for engines with single injection and small EGR because in that conditions the fraction of thermal NO is main and prompt NO may not be accounted.

CONCLUSION

The presented RK-model is intended for diesel combustion simulation. It takes into account and allows optimization of: piston bowl shape, injector design and location, shape of injection profile including multiple injection. The RK-model accounts for: drop sizes, interaction of free sprays with swirl, spray and wall impingement, evolution of near-wall flow formed by spray, hit of fuel on cylinder head surface, hit of fuel on cylinder liner, crossing of NWF formed by adjacent sprays, effect of piston motion and swirl intensity on heat release rate. The multi-zone RK-model takes into account EGR, temperatures of piston and cylinder head in heat release computation. The model allows prediction of heat release rate, NOx and smoke emission for different kinds of diesels working over the whole operating range without recalibration. The ability to predict diesel parameters with high accuracy for different kinds of injection profile including multiple injection with large injection timing (PCCI), allows this model to be used for development of the Common Rail system controlling algorithm. The RK-model allows designing of piston bowl shape, selection of injector holes numbers, diameters and directions in match with swirl intensity to control emission and fuel consumption. The RK-model includes Detail Kinetic Mechanism for both prompt and thermal NOx simulation.

The RK-model does not require powerful computer. Simulation of combustion at single injection requires 5-7 seconds on conventional laptop. Computational time at double injection is about 10-12 seconds. The fast simulation allows use the RK-model together with optimization software for search the optimal combination of engine data to provide small level of emissions and SFC.

The use of the procedures of multiparametric optimization in combination with the accurate and high-speed computer model of an engine enables the efficiency of computational research to be radically increased.

ACKNOWLEDGMENTS

The author was fortunate to have as the mentor and colleague Prof. N. Razleytsev (1934-2003), whose contribution has been the base of the developed software. Also, the author would like to acknowledge contributions of his colleagues at BMSTU, in particular Dr. Nikolay Ivaschenko and Dr. Leonid Grekhov, for their support of this research as well as Dr. Andrey Kozlov and Mr. Yuriy Fadeyev for their work in DIESEL-RK development.

REFERENCES

1. Kuleshov, A.S. Use of Multi-Zone DI Diesel Spray Combustion Model for Simulation and Optimization of Performance and Emissions of Engines with Multiple Injection. 2006, SAE Paper No 2006-01-1385.
2. Kuleshov, A.S. Multi-Zone DI Diesel Spray Combustion Model and its application for Matching the Injector Design with Piston Bowl Shape. 2007, SAE Paper No 2007-01-1908.
3. A. Kuleshov and K. Mahkamov Multi-zone diesel fuel spray combustion model for the simulation of a diesel engine running on biofuel // Proc. Mechanical Engineers Vol. 222, Part A, Journal of Power and Energy. 2008. pp. 309 – 321.
4. Zeldovich Ya.B., Raizer Yu.P.: "Physics of shock waves and high-temperature hydrodynamic phenomena", Moscow: Nauka, 686 p., 1966. (In Russian).

5. Zvonov V.A.: “Internal combustion engines toxicity”, Moscow: Mashinostroenie, 200 p., 1973. (In Russian).
6. Razleytsev N.F.: “Combustion simulation and optimization in diesels”, Kharkov: Vischa shkola, 169 p., 1980. (In Russian).
7. Miller J.A., Bowman C.T. Mechanism and modeling of nitride. Chemistry in Combustion // Prog. Energy Combustion Science. – 1989. – v.15. – P.287-338.
8. Bochkov M.V., Lovachev L.A., Hvisevich S.N. Formation of the Nitrogen Ox-ide (NO) at Laminar Flame Propagation in the Homogeneous Air-Methane Mixture // FGV – vol. 34 – 1998. – No 1. (in Russian).
9. Bochkov M.V., Lovachev L.A., Hvisevich S.N. Numerical Modeling the NOx Formation at Air-Methane Mixture Combustion at Condition of Coupled Processes of Chemistry Kinetic and Molecules Diffusion // Mathematical Modeling. – 1997. – No3. – vol. 9. – pp. 13-28. (in Russian).
10. Kamimoto, T., Kobayashi, H., and Matsuoka, S.: “A Big Size Rapid Compression Machine for Fundamental Studies of Diesel Combustion”, SAE Paper 811004, SAE Trans., vol. 90, 1981.
11. Reitz, R.D. and Bracco, F.V.: “On the dependence of Spray Angle and Other Spray Parameters on Nozzle Design and Operating Conditions”, SAE paper 790494, 1979.
12. Bracco, F.V.: “Modeling of Engine Sprays”, SAE Paper No 850394, 1985.
13. Kuo, T.W. and Bracco, F.V.: “Computations of Drop Sizes in Pulsating Sprays and of Liquid-Core Length in Vaporizing Sprays”, SAE Paper No 820133, SAE Trans., vol. 91, 1982.
14. Kaluzhin S.A., Romanov S.A., Sviridov Yu.B.: “Experimental investigation into velocities of liquid and gaseous phases in diesel fuel flame”, Dvigatelestroenie, No. 7, pp. 5-8, 1980. (In Russian).
15. Lyn, W.T.: “Study of Burning Rate and Nature of Combustion in Diesel Engines”, in Proceedings of Ninth International Symposium on Combustion, pp. 1069-1082, The Combustion Institute, 1962.
16. Heywood, J.B.: Internal Combustion Engine Fundamentals, McGraw-Hill, New York, 1988.
17. Dragunov G.D., Egorov V.V.: “Some peculiarities of fuel moving along the combustion chamber surface”, Izv. Vuzov, Mashinostroenie, No. 1, pp. 119-122, 1977. (In Russian).
18. Egorov V.V.: “Investigation into peculiarities of fuel evaporation and working cycle in boosting the tractor diesel with the CNIDI combustion chamber”, Ph. D. Thesis, Leningrad, 1978. (In Russian).
19. Ivanchenko N.N., Semenov B.N., Sokolov V.S.: “Working process in diesels with piston bowl”, Leningrad, Mashinostroenie, 228 p., 1972. (In Russian).
20. Novoselov V.D.: “Investigation into working process of four-stroke diesels based on ChN26/26 engines with mean effective pressure above 20 kg/cm^2 with limitations on maximum combustion pressure”, Ph. D. Thesis, Leningrad, 1978. (In Russian).
21. Semenov B.N.: “Theoretical and experimental fundamentals of applying fuels with various physical and chemical properties in high-speed diesels”, Dr. Snc. Thesis, Leningrad, 1978. (In Russian).
22. Sokolov S.S., Demidova N.I., Safonov V.K.: “Increase of diesel reliability by optimization of combustion chamber”, Energomashinostroenie, No. 2, pp. 12-14, 1973. (In Russian).
23. Semenov B.N., Pavlov E.P.: “Investigation and development of volume and film fuel-air mixing in diesels”, Energomashinostroenie, No. 1, pp. 7-10, 1978. (In Russian).
24. Balles, E.: “Fuel-Air Mixing and Diesel Combustion in a rapid Compression Machine”, Ph.D. Thesis, Department of Mechanical Engineering, MIT, June 1987.
25. Gavrilov V.V.: “Methods increasing quality of fuel-air mixing and combustion in a marine diesel based on mathematical and physical simulation of local intracylinder processes”, Dr. Snc. Thesis, Saint Petersburg, StPb SMTU, 2004. (In Russian).
26. Lyshevsky A.S.: “Fuel atomization in marine diesels”, Leningrad, 248 p., 1971. (In Russian).
27. Kuo, T.W., and Bracco, F.V.: “On the Scaling of Transient Laminar, Turbulent and Spray Jets”, SAE Paper No. 820038, 1982.
28. Hiroyasu, H., Kadota, T and Arai, M.: “Supplementary Comments: Fuel Spray Characterization in Diesel Engines”, Combustion Modeling in Reciprocating Engines, Ed. By Mattavi, J.N. and Amann, C.A., pp. 369 – 408, Plenum Press, N.Y., 1980.
29. Arregle, J., Pastor, J.V. and Ruiz, S. The Influence of Injection Parameters on Diesel Spray Characteristics. 1999, SAE Paper No. 1999-01-0200, 1999.
30. Pastor, J.V., Encabo, E. and Ruiz, S. New Modelling Approach for Fast Online Calculations In Sprays. 2000, SAE Paper No. 2000-01-0287.
31. Larmi, M., Rantanen, P., Tiainen, J., Kiijarvi, J., Tanner, F.X. and Stalsberg-Zarling, K. Simulation of Non-Evaporating Diesel Sprays and Verification with Experimental Data. 2002, SAE Paper No. 2002-01-0946.
32. Nakagawa, H., Oda, Y., Kato, S., Nakashima, M and Tateishi, M. Fuel Spray Motion in Side Injection Combustion System for Diesel Engines. Proceedings of the International Symposium COMODIA 90, 1990, 281-286.
33. Reitz, R. D. and Bracco, F. B. On the Dependence of Spray Angle and Other Spray Parameters on Nozzle Design and Operating Conditions // SAE Paper 790494, 1979.
34. Dan T. The Turbulent Mechanism and Structure of Diesel Spray. Ph. D. Thesis, Toshisya University, 1996.
35. Dohoy Jung and Dennis N. Assanis. Multi-zone DI Diesel Spray Combustion Model for Cycle Simulation Studies of Engine Performance and Emissions // SAE Paper No 2001-01-1246, 2001.

36. Hiroyasu, H., and Arai, M. Fuel Spray Penetration and Spray Angle of Diesel Engines // Trans. of JSAE, Vol. 21, 1980, pp. 5-11.
37. Sviridov Yu.B., Malyavsky L.V., Vihert M.M.: “Fuel and fuel supply in automotive diesels”, Leningrad, 224 p., 1972. (In Russian).
38. Tolstov A.I. Indicated period of ignition lag and dynamic of cycle of high speed engine with compression ignition. // Tr. NILD "Research of working cycle and fuel supply in the high speed diesels". N1. M.: Mashgiz, 1955. pp. 5-55. (In Russian).
39. Marco Bakenhus and Rolf D. Reitz: “Two-Color Combustion Visualization of Single and Split Injections in a Single-Cylinder Heavy-Duty D.I. Diesel Engine Using an Endoscope-Based Imaging System”, SAE Paper No. 1999-01-1112, 1999.
40. Soon-Ik Kwon, Masataka Arai, Hiroyuki Hiroyasu: “Ignition Delay of a Diesel Spray Injected Into a Residual Gas Mixture”, SAE Paper No. 911841, 1991.
41. Schneider W., Stockli M., Lutz T., Eberle M. Hochdruckeinspritzung und Abgasrezirkulation im kleinen, schnellaufenden Dieselmotor mit direkter Einspritzung. MTZ. N 11, 1993. S.588-599.
42. Hisashi Akagawa, Takeshi Miyamoto, Akira Harada, Satoru Sasaki, Naoki Shimazaki, Takeshi Hashizume, Kinji Tsujimura "Approaches to solve problems of the premixed lean diesel combustion". SAE Pap No 1999-01-0183, 1999, 13 p.
43. Akira Harada, Naoki Shimazaki, Satoru Sasaki, Takeshi Miyamoto, Hisashi Akagawa and Kinji Tsujimura "The Effect of Mixture Formation on Premixed Lean Diesel Combustion Engine". SAE Pap No 980533, 1998, 10 p.
44. Yoshiaki Nishijima, Yasuo Asaumi, Yuzo Aoyagi "Premixed lean diesel combustion (PREDIC) using impingement spray system". Sae Pap No 2001-01-1892, 2001, 9 p.
45. Wartsila. Technology review: (http://www.wartsila.com/Wartsila/global/docs/en/ship_power/media_publications/brochures/product/engines/w46_tr.pdf)
46. X. He, M.T. Donovan, B.T. Zigler, T.R. Palmer, S.M. Walton, M.S. Wooldridge, A. Atreya "An Experimental and modeling study of iso-octane ignition delay times under homogeneous charge compression ignition conditions" // Combustion and Flame, 142 (2005) 266-275.
47. Hardenberg H.O. and Hase F.W. Empirical Formula for Computing the Pressure Rise Delay of a Fuel from its Cetane Number and from the Relevant Parameters of Direct-Injection Diesel Engines // SAE Paper 790493, 1979.
48. Gary D. Neely, Shizuo Sasaki, Jeffrey A. Leet "Experimental investigation of PCCI-DI combustion on emissions in a light-duty diesel engine", SAE Pap No 2004-01-0121, 2004, 11 p.
49. Kazuhisa Inagaki, Takayuki Fuyuto, Kazuaki Nishikawa, Kiyomi Nakakita, Ichiro Sakata "Combustion System with Premixture-controlled Compression Ignition". Research Report R&D Review of Toyota CRDL Vol. 41, No 3, 2006, pp 35-46.
50. Wanhua Su, Tiejian Lin, Yiqiang Pei "A compound technology for HCCI combustion in a DI diesel engine based on the multi-pulse injection and the BUMP combustion chamber". SAE Pap No 2003-01-0741, 2003, 10 p.
51. Ryo Hasegawa, Hiromichi Yanagihara "HCCI combustion in DI diesel engine" SAE Pap No 2003-01-0745, 2003, 8 p.
52. http://www.diesel-rk.bmstu.ru
53. A.S. Kuleshov: “Model for predicting air-fuel mixing, combustion and emissions in DI diesel engines over whole operating range”, SAE Paper No 2005-01-2119, 2005.
54. http://www.iosotech.com

CONTACT

Dr. Andrey Kuleshov,
Piston Engine Department of Bauman Moscow State Technical University,
2-Baumanskaya, 5, 105005, Moscow, Russia,
Tel.: +7(495) 265-78-92
e-mail: kuleshov@power.bmstu.ru
http://www.diesel-rk.bmstu.ru

ABBREVIATIONS

CA: Crank angle.

CFD: Computational Fluid Dynamic

DI: Direct Injection.

DKM: Detail Kinetic Mechanism intended for correct prediction of NO emission in engine with large EGR, multiple injection and PCCI/HCCI. DKM includes 199 reactions with 33 species.

EFM: Elementary Fuel Mass injected at one time step (increment).

EGR: Exhaust Gas Recirculation

FSV: Fuel Spray Visualization is software intended for the analysis of the animation picture of interaction of fuel sprays with the combustion chamber walls, with swirl and among themselves. The code helps to design the shape of a piston bowl and select correctly the diameter, the number and the directions of injector nozzles according to concrete injection profile and swirl intensity.

HCCI: Homogeneous Charge Compression Ignition.

HTC: High Temperature Combustion.

IOSO: Intelligent Optimization Self Organization is a general computer code for non linear optimization.

LTC: Low Temperature Combustion

NWF: Near Wall Flow formed after spray-wall impingement is a flow of air and fuel droplets spread

along the surface of piston or cylinder liner of cylinder head.

PCCI: Premixed Charge Compression Ignition.

PM: Particulate Matter emission.

SFC: Specific Fuel Consumption.

SOC: Start of combustion (CA deg. before TDC).

SOI: Start of injection (CA deg. before TDC).

NOMENCLATURE

b_{ui} : Evaporation constant for i-zone.

b_m : Depth of spray forward front, m.

C : EGR fraction in the cylinder.

C_C : Correction factor accounting composition of air charge.

C_T : Correction factor accounting for temperature growth rate in the auto-ignition delay period.

d_{32} : Sauter mean diameter, m.

D_{po} : Diffusion factor of fuel under atmospheric conditions, s.

D_p : Diffusion factor for fuel vapor under combustion chamber conditions, s.

d_k : Current diameter of drop, m.

d_l **:** diameter of large drops of fuel, m.

d_n : Nozzle hole diameter, m.

d_0 : Initial diameter of drop; m.

dx/dj : Heat release rate, 1/deg.

dx/dt: Heat release rate, 1/sec.

dt : time step, sec.

dQ : time step at autoignition calculation, CA deg.

dj : time step, CA deg.

h_{clr} : Piston-head clearance depended on CA, m.

l_{wj} : Dimensions of NWF spot in each directions, m.

K_i : Theoretical evaporation constant in the i-zone.

K_j : Factor of form of NWF.

l : Current distance between the injector's nozzle and the EFM, m.

l_m : EFM's penetration distance, m.

M : Square of Ohenzorge number.

m_f : Cycle fuel mass.

n : engine speed [RPM].

Nu_D : e Nusselt number for diffusion process.

p_S : Pressure of saturated fuel vapor.

r_f : Density of liquid fuel, kg/m^3

P_{inj} : Injection pressure.

$P_{inj\,max}$: Maximum injection pressure.

p : pressure in the cylinder.

S : piston stroke, m.

T_k : Effective temperature of zone inside NWF depending on the corresponding wall temperature, K.

U : Current velocity of the EFM, m/s.

U_o : Initial velocity of the EFM at the nozzle of the injector, m/s.

T_{wi} : Wall temperature, K.

V_{inj} : Injection velocity, m/s.

V : In-cylinder volume, Zone volume, m^3.

V_i : Cylinder volume at beginning of HTC of current fuel portion m^3.

V_c : Cylinder volume at TDC, m^3.

p : In-cylinder pressure.

R_s : Swirl ratio.

R : cylinder radius, m.

r_V : Relative evaporation rate in the zones of outer sleeve and front.

r_{Wi} : Relative evaporation rate in different NWF zones.

T : Temperature, K.

T_{Wi} : Wall temperature of a corresponding zone, K.

U : Current velocity of EFM, m/s.

U_{0m} : Average injection velocity, m/s.

U_t : Tangential velocity of EFM in the swirl direction, m/s.

We : Weber number.

W_t : Local tangential air velocity, m/s.

x : Fraction of burnt fuel.

x_t : Temperature growth rate at the auto-ignition delay period, K/sec.

Y : Empirical correction function.

y_S : Correction factor depending on piston stroke.

y_{RPM} : Correction factor taking into account engine speed.

y_{O2} : Concentration of oxygen in the Michigan University self ignition delay equation.

a : A/F equivalence ratio in the cylinder.

g : Spray angle, rad.

g_j : Impingement angles, rad.

Δy_j : Deformation of generating lines of the spray by swirl in windward Δy_3 and leeward Δy_4 directions, m.

x_b : Efficiency of in-cylinder air use.

f : Function describing completeness of fuel vapor combustion in the zones.

f : Air fuel ratio in the Michigan University self ignition delay equation.

j : Crank Angle used at combustion simulation.

j_z : Combustion duration in CA deg.

m_f : Dynamic viscosity coefficient of fuel, Pa s.

r : Dimensionless density.

r_{air} : Air density, kg/m^3.

r_f : Fuel density, kg/m^3.

t : Time, sec.

t_s : Current time from the injection beginning, s.

$t_{s\,max}$: Time of the spray evolution, sec.

t_i : Auto-ignition delay period, sec.

t_{inj} : Injection duration, sec.

t_k : Travel time for the EFM to reach a distance l from the injector's nozzle, s.

t_m : Travel time for the EFM to reach a distance l_m from the injector's nozzle, s.

t_{sw} : Time of arrival of spray to wall, s.

t_w : Time of evolution of NWF along the wall, s.

t_{s0i} : Time of arrival of fuel into i–zone, s.

t_{iT} : Auto-ignition delay period calculated as a function of current pressure, and temperature, sec.

t_{ign} : Auto-ignition delay period calculated as a function of current pressure, temperature and composition, sec.

t_u : Current time from evaporation beginning, s.

t_{lburn} : Time of evaporation and combustion of large drops of fuel, sec.

Θ: Crank Angle used at ignition delay calculation.

Θ_i : Auto-ignition delay period, CA deg.

s : Fraction of fuel.

s_f : Fuel surface density, N/m.

s_u : Fraction of fuel evaporated up to the current moment.

s_{ud} : Fraction of fuel evaporated during ignition delay period.

s_{ui} : Fraction of fuel evaporated up to the current moment in the i-zone.

s_{zi} : Fuel fraction in the i–zone.

ν : Air kinematics viscosity.

χ : Swirl damping factor.

ω : Angular velocity of swirl, rad/s.

ω_C : Angular velocity of crank, rad/s.

$\Im$: Dimensionless criterion.

SUBINDEXES

air : Air

a : Initial site of the spray forming.

b : Main site of the spray evolution.

core : Dense core of free spray.

crone : Crone of piston.

cross : Zones of NWF crossing.

env : Dilute outer sleeve.

f : Fuel.

front : Forward front of free spray.

head : Cylinder head.

g : Border between Initial site of the spray forming and main site of spray evolution.

j =1 : radial direction from cylinder center to liner.

j =2 : radial direction from liner to cylinder center.

j =3 : tangential on wind direction.

j =4 : tangential down wind direction.

liner : Cylinder liner.

k : Control section.

m : section behind forward front.

s : Spray tip section.

w : Near wall flow.

w env : Dilute outer surrounding of NWF.

w fr : Forward front of NWF.

w core : Dense core of NWF.